OR1992_25 1,41

Tasmania Department Of Mines — Report 1992/25

Gravity gradients at several Tasmanian sites

by R. G. Richardson

Abstract

Data from the Que–Hellyer, Oceana and Fingal Tier areas were used to compute the horizontal and vertical derivatives of the Bouguer anomaly. With the exception of the Que River detailed area, the first derivatives were generally less than 10 mgal/km. Except in areas of well known geology with targets having near-vertical density boundaries and large horizontal and vertical extents, the measurement of only gradient data serves to increase the difficulties of qualitative and quantitative interpretation.

INTRODUCTION

Early gravity measurements made under laboratory conditions using pendulums were accurate to ±2 mgal. It was recognised at the time that this would be of no use for field surveys over small features and methods were developed to measure the horizontal gradients of gravity to an accuracy of ±0.1 mgal/km. The Imperial Geophysical Experimental Survey of 1928–30 (Edge and Laby, 1931) carried out the first reported gravity surveys in Australia and presented a detailed discussion of the corrections required and the limitations involved. In summary corrections are required for close terrain effects (for which levels were taken with an accuracy of 0.3 m to a radius of 30 m), topographic effects (for which a plan contoured at intervals of 1.5 m between radii of 30 m and 300 m was used), and other features such as buildings, cuttings, embankments and trees. Edge and Laby state that "the principal use of the (gravity gradient) method is in the location and investigation of geological structures, such as faults, anticlines, synclines, domes, etc. Its application to metalliferous deposits is rather limited, as in the majority of cases the lodes are too small or occur in rugged or mountainous country where the method could only be applied with great difficulty or not at all". The results were presented either as contours of gradient magnitude, as in this report, or as vectors which point in the direction of a more dense body.

Stanley and Green (1976) presented a method for locating large truncated plates and geologic contours by measuring the horizontal gravity gradient and calculating the vertical gradient from this. They suggest that a measurement base of 100 ± 5 m (true horizontal distance) is required for a 10 microgal accuracy instrument. Although the absolute meter elevation is not required, corrections must still be made for the difference in meter elevation and terrain correction between the two reading positions making up a gradient measurement, and for differences in latitude. For a 10 μgal accuracy instrument this corresponds to a height accuracy of ±2.5 cm and a terrain correction accuracy of ±0.01 mgal.

Recent developments in gravity meter technology (e.g. the Scintrex CG-3M with an accuracy of 5 μgal) raise the possibility of direct measurement of both horizontal and vertical gravity gradients. For horizontal measurements this corresponds to determining the elevation difference to ±1.25 cm and the terrain correction to ±0.005 mgal. For vertical gradient measurement the height difference may be rigidly fixed but the terrain correction value at each meter position requires determination to ±0.005 mgal. If the suggested meter spacing of one metre is adopted, the minimum vertical gradient resolvable would be 10 mgal/km (= 10 μgal/m).

The GPC package from Exploration Computer Services allows the calculation of horizontal and vertical derivatives, and it was decided to apply this package to several existing data sets to determine the amplitudes of the gradients and look at the enhancement of known geological features. The following public data sets were selected:

(i) Que–Hellyer Area — regional coverage with a mixture of barometric heighting and surveyed levels.

(ii) Que River Area — detailed coverage with surveyed levels.

(iii) Hellyer Area — detailed coverage with surveyed levels.

(iv) Oceana General — regional coverage with a mixture of barometric heighting and surveyed levels.

(v) Oceana Detail — detailed coverage with surveyed levels.

(vi) Fingal Tier — regional coverage with barometric heighting. An area containing a number of large amplitude areally extensive features associated with dolerite feeders and structures.

RESULTS

(i) Que–Hellyer area

The area is covered by stations at a one kilometre nominal spacing with more detailed coverage over the two mines (fig. 1). The Bouguer Anomaly data were gridded with a 100 m mesh (fig. 2) and then filtered with a 600 m radius Gaussian filter (fig. 3). Interestingly the Que River and

Hellyer ore bodies are both located on the one isolated gravity high.

The east-west gradient of the raw Bouguer Anomaly (fig. 4) shows a number of elongate anomalies corresponding to the main gradients on the Bouguer Anomaly plot, as would be expected, and a very noisy area over the Que River Mine suggesting that the positions read may not have been precisely those levelled several years earlier. The east-west, north-south and vertical gradients of the filtered Bouguer Anomaly are shown in Figures 5, 6 and 7 respectively. Figure 8 presents the 3-D analytic signal (the magnitude of the vector of the total gradient). Gradients of up to 13 mgal/km are present.

(ii) Que River area

The area is covered by stations at either 25 × 50 m or 50 × 100 m nominal spacing. The Bouguer Anomaly data were gridded with a 25 m mesh (fig. 9) and then filtered with a 100 m radius Gaussian filter. The east-west, north-south and vertical gradients of the filtered Bouguer Anomaly are shown in Figures 10, 11 and 12 respectively. Figure 13 presents the 3-D analytic signal. The vertical gradient has values up to 40 mgal/km.

(iii) Hellyer Area

The area is covered by stations on a 50 × 100 m nominal spacing. Levelling was carried out at the time of reading. The Bouguer Anomaly data were gridded with a 25 m mesh (fig. 14) and then filtered with a 100 m radius Gaussian filter. The east-west, north-south and vertical gradients of the filtered Bouguer Anomaly are shown in Figures 15, 16 and 17 respectively. Figure 18 presents the 3-D analytic signal. The vertical gradient has values up to 16 mgal/km.

(iv) Oceana General

The area is covered by barometrically levelled stations at 1 km and 0.46 km nominal spacings, with a more detailed coverage on a number of mineral exploration grids (fig. 19). The Bouguer Anomaly data were gridded with a 100 m mesh (fig. 20) and then filtered with a 300 m radius Gaussian filter (fig. 21). The east-west, north-south and vertical gradients of the filtered Bouguer Anomaly are shown in Figures 22, 23 and 24 respectively. Figure 25 presents the 3-D analytic signal. The vertical gradient has values up to 16 mgal/km.

(v) Oceana Detail

The area is covered by stations at either 25 × 25 m, 50 × 50 m, or 50 × 100 m nominal spacings. Although the stations have been accurately levelled, positioning is only approximate and terrain correction was performed without the benefit of either accurate positions or near-zone terrain descriptions. The Bouguer Anomaly data were gridded with a 25 m mesh (fig. 26) and then filtered with a 100 m radius Gaussian filter. The calculated gradient data were also filtered with a 100 m radius Gaussian filter. The filtered east-west, north-south and vertical gradients of the Bouguer Anomaly are shown in Figures 27, 28 and 29 respectively. Figure 30 presents the 3-D analytic signal. The vertical gradient has values up to 40 mgal/km.

(vi) Fingal Tier

The area is covered by barometrically levelled stations with spacings varying between 200 m and greater than 1.5 km (fig. 31). The Bouguer Anomaly data were gridded with a 100 m mesh (fig. 32) but not filtered. There is a strong correlation between the Bouguer Anomaly and the known dolerite structures. The calculated gradient data were filtered with a 500 m radius Gaussian filter. The filtered east-west, north-south and vertical gradients of the Bouguer Anomaly are shown in Figures 33, 34 and 35 respectively. Figure 36 presents the 3-D analytic signal. The vertical gradient has values up to 30 mgal/km.

The presentation of gradient data most commonly used by Edge and Laby (1931) was vector format, in which the arrows pointed in the direction of a more dense body. As an alternative to the contour presentation used throughout this report it was decided to produce a traditional vector diagram for the Fingal Tier data set. The vector directions and magnitude were calculated from the east-west and north-south smoothed gradient data. Figure 37 presents the vectors for data points on a 200 m mesh and Figure 38 presents the vector for data points on a 100 m mesh. Any vector with a length of less than twice the diameter of the arrow head was not plotted. The vectors clearly outline the edges of the major dolerite bodies.

DISCUSSION

(i) Que–Hellyer Area

As noted earlier, the Que River and Hellyer ore bodies are located on an isolated gravity high. The Que River portion of the high corresponds to an area of pyritic and sericitic alteration (Komyshan, 1988) but there are similar areas mapped that do not fall on the high. The closed high at Hellyer has no obvious source on the available geological maps. On the 3-D analytic signal (fig. 8) the major east-west feature at approximately 393 200 mN corresponds, in part, to a mapped fault. Similarly the north-south feature at approximately 391 500 mE, 391 000 mN corresponds to the position of the Henty Fault Zone as mapped by Komyshan. This same feature can be continued north to 398 700 mN. When viewed in isolation, the Que River and Hellyer data show little correlation with the geology. The north-south feature described in Figure 8 is seen on Figures 9, 12 and 13, as well as a number of the data presentations in Leaman and Richardson (1981*a*).

(ii) Oceana area

The Bouguer Anomaly in this area (fig. 20) is dominated by a strong NW-SE trend. There is a negative feature in the Mt Zeehan area on the southeastern side of the mountain that coincides with the Oceana Fault. The closed negative feature centred at 362 700 mE, 359 000 mN is over an area mapped as Crotty Quartzite and Florence Quartzite (Blissett and Gulline, 1962).

When the geological map is overlain by the vertical derivative plot (fig. 24) the major features are seen to be associated with the Oceana, Balstrup and Pyramid Faults, with an un-named fault running through the Comstock and Brittania areas, and with the Florence Quartzite in the

North Austral area. The anomaly near Mt Zeehan is not easily explained.

(iii) Fingal Tier

The structure of the Fingal Tier area is dominated by a number of dolerite feeders as shown in Leaman and Richardson (1981*b*, p.52). The vector gravity gradient plots (fig. 37 and 38) clearly delineate the major feeders as areas of high density (vectors pointing in), and for this aspect are much more easily interpreted than any of the contour plots from the area. The Bouguer Anomaly, vertical gradient and 3-D analytic signal plots (fig. 32, 35 and 36) all show a major feature commencing at about 591 000 mE, 381 000 mN and running along a bearing of about 340° (grid). This corresponds to a line of dolerite feeders but also lines up with the "gold belt", and may represent an extension of this (D. E. Leaman, pers. comm.).

REFERENCES

BLISSETT, A. H.; GULLINE, A. B. 1962. One mile geological map series. K/55-5-50. Zeehan. *Department of Mines, Tasmania.*

EDGE, A. B. B.; LABY, T. H. 1931. *The principles and practice of geophysical prospecting.* Cambridge University Press.

KOMYSHAN, P. 1986. Geology of the Mt Charter–Hellyer area. *Geol. Map Mt Read Volcanics Proj. Tasm.* 1.

LEAMAN, D. E.; RICHARDSON, R. G. 1981*a*. Gravity survey of the Que River deposit, western Tasmania. *Unpubl. Rep. Dep. Mines Tasm.* 1981/24.

LEAMAN, D. E.; RICHARDSON, R. G. 1981*b*. Gravity survey of the East Coast coal fields. *Bull. geol. Surv. Tasm.* 60.

STANLEY, J. M.; GREEN, R. 1976. Gravity gradients and the interpretation of the transacted plots. *Geophysics* 41:1370–1376.

[21 August 1992]

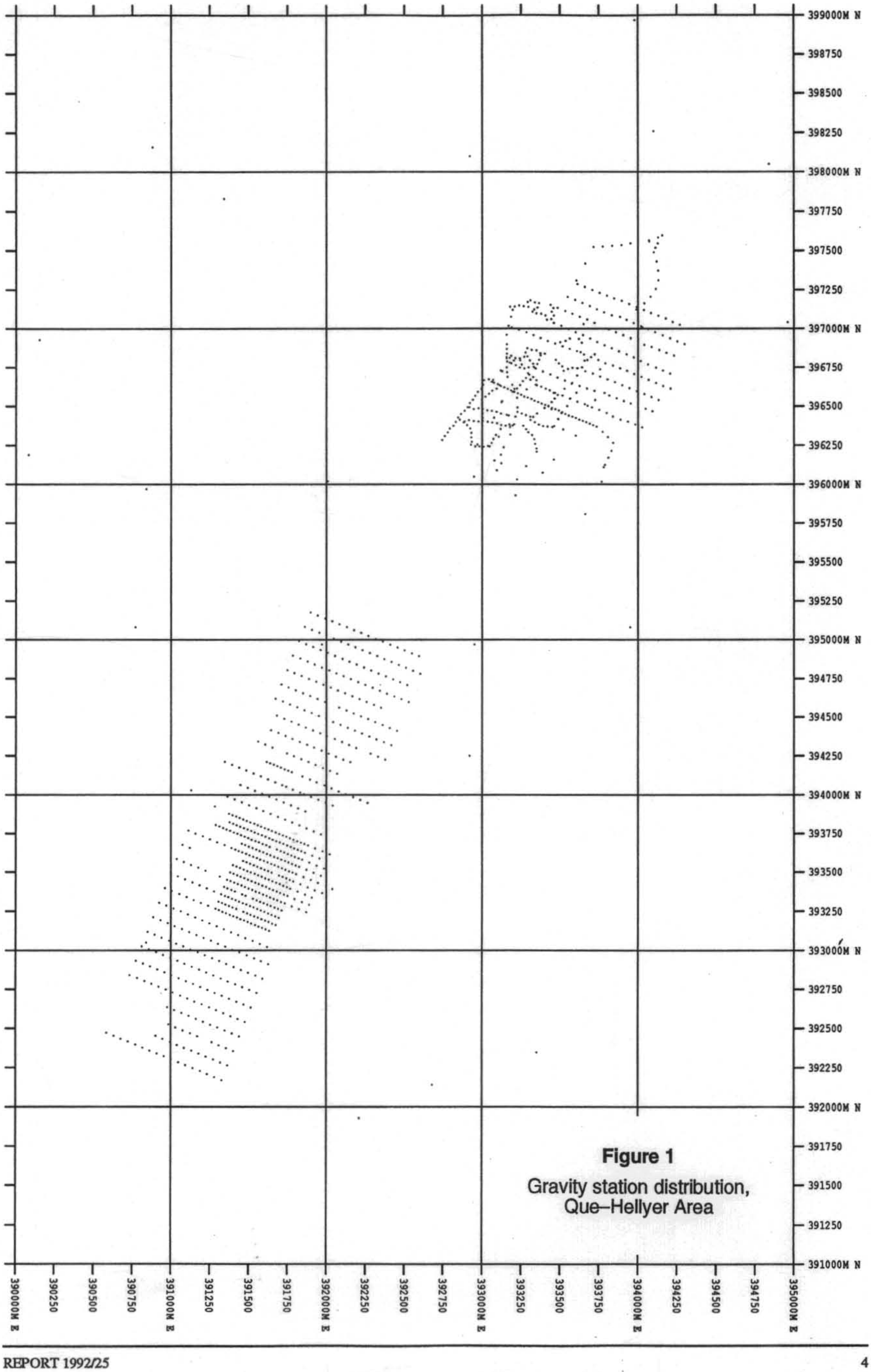

Figure 1

Gravity station distribution, Que–Hellyer Area

5/41

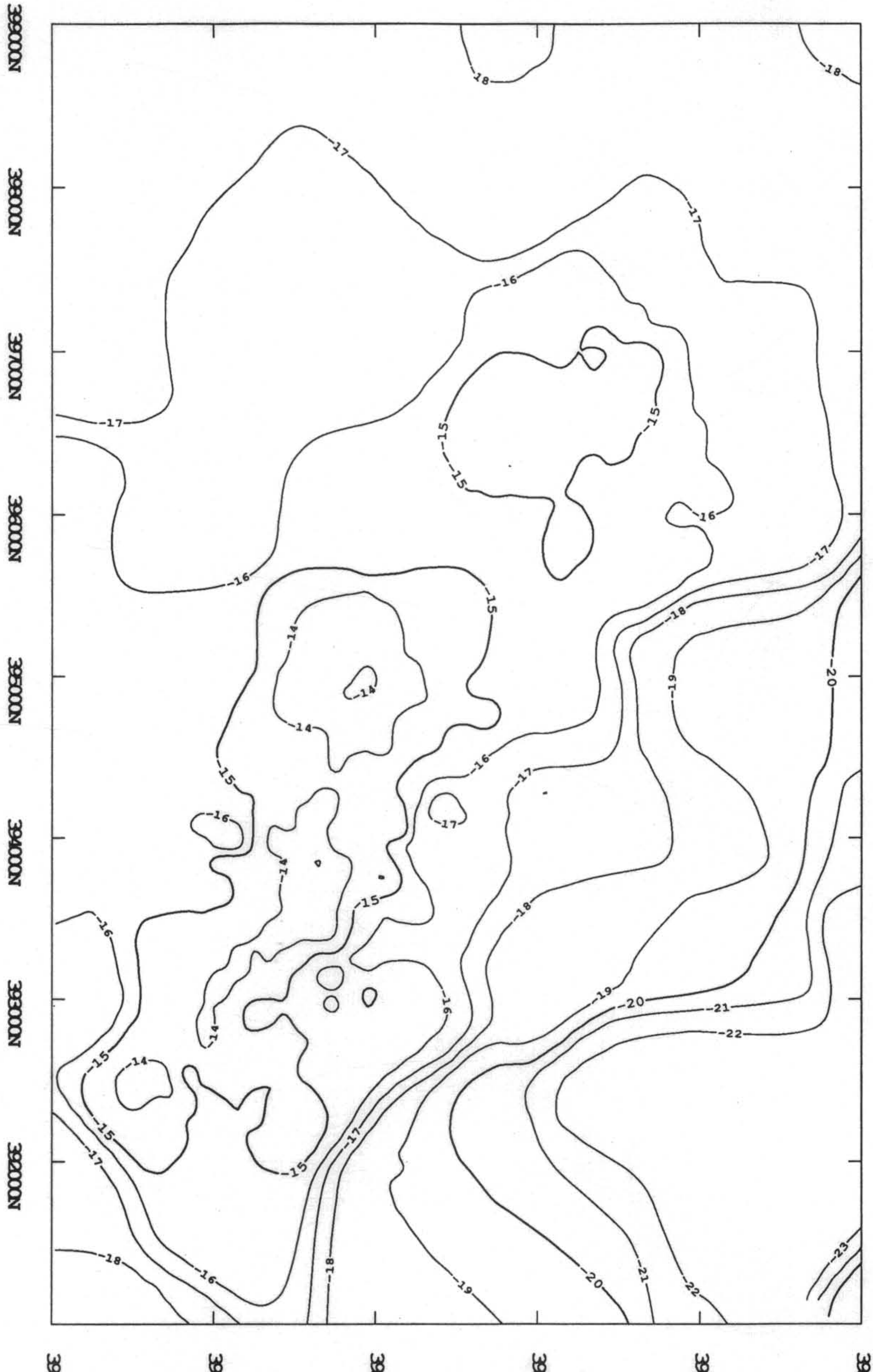

Figure 2

Raw Bouguer Anomaly, Que–Hellyer Area

5 cm

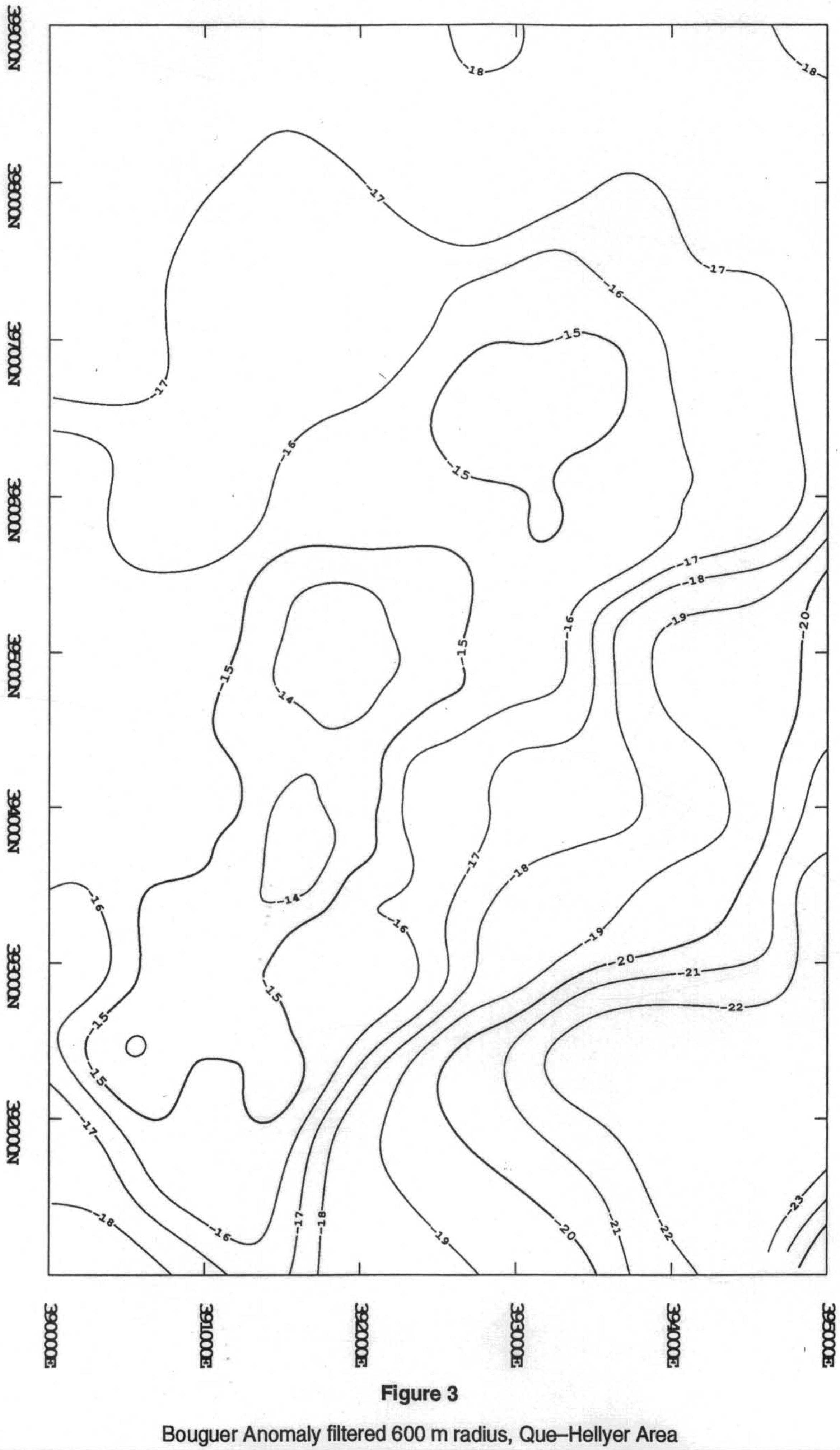

Figure 3

Bouguer Anomaly filtered 600 m radius, Que–Hellyer Area

5 cm

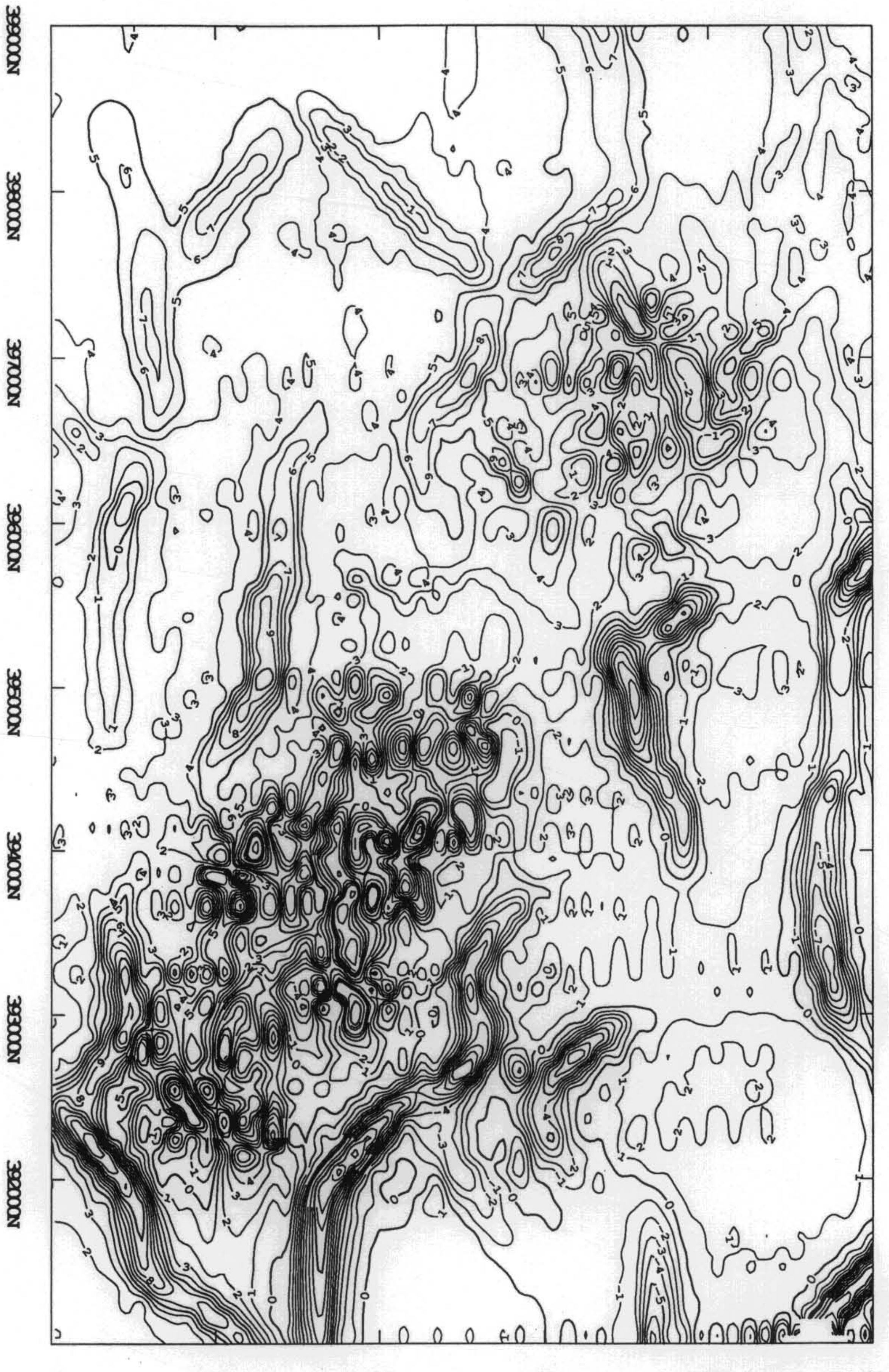

Figure 4

East-west gradient of raw Bouguer Anomaly, Que–Hellyer Area

5 cm

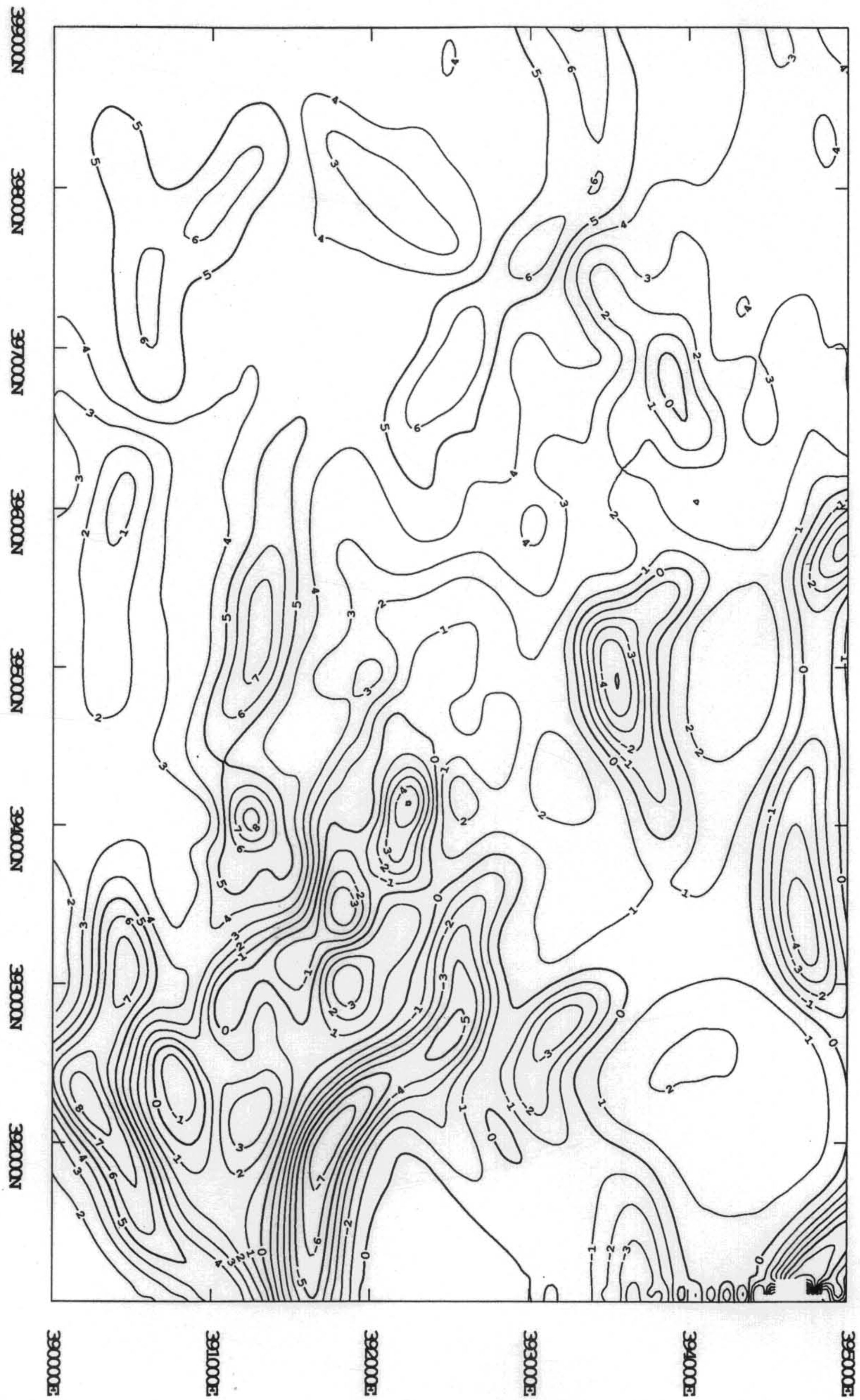

Figure 5

East-west gradient of filtered Bouguer Anomaly, Que–Hellyer Area

5 cm

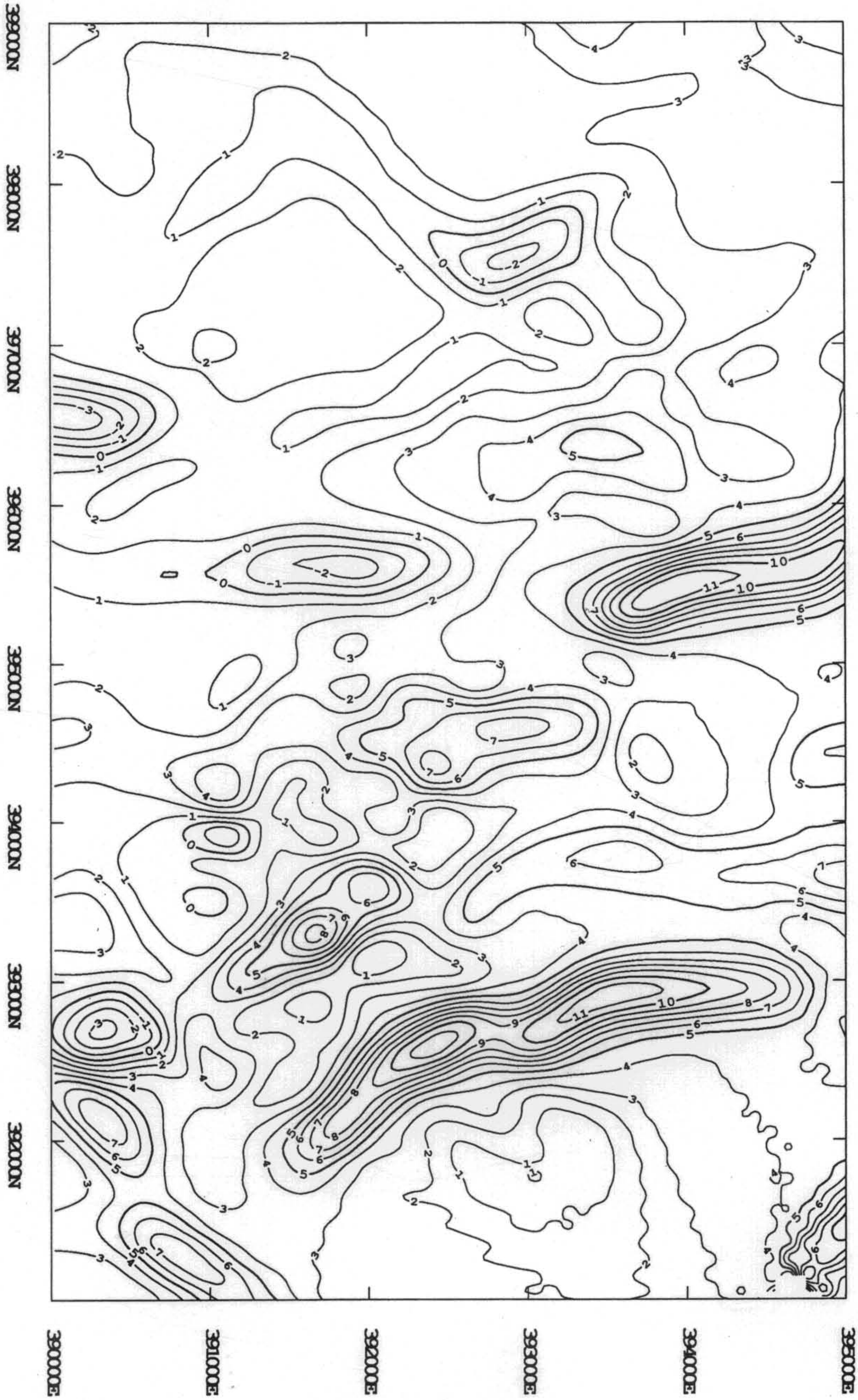

Figure 6

North-south gradient of filtered Bouguer Anomaly, Que–Hellyer Area

5 cm

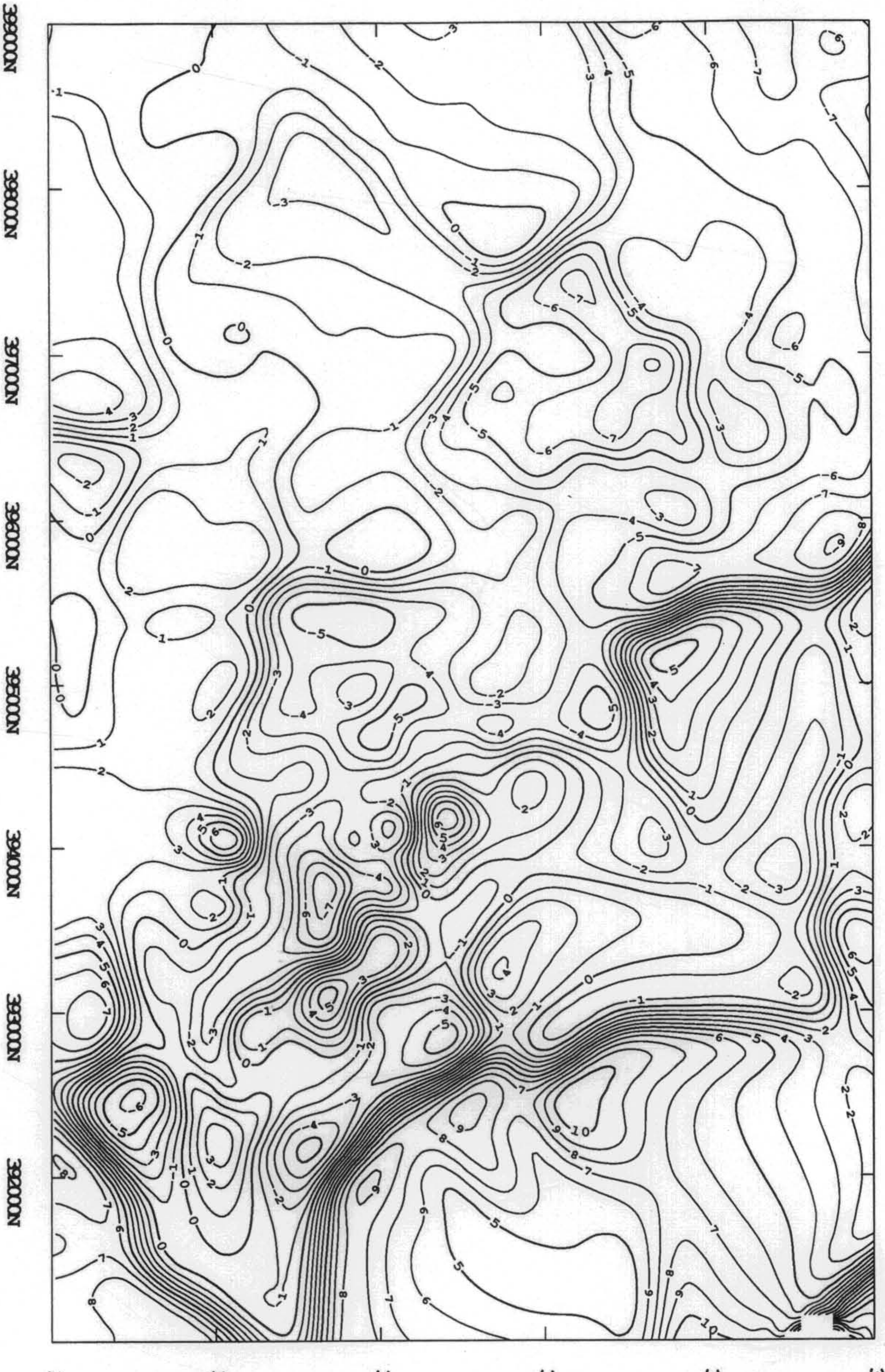

Figure 7

Vertical gradient of filtered Bouguer Anomaly, Que–Hellyer Area

5 cm

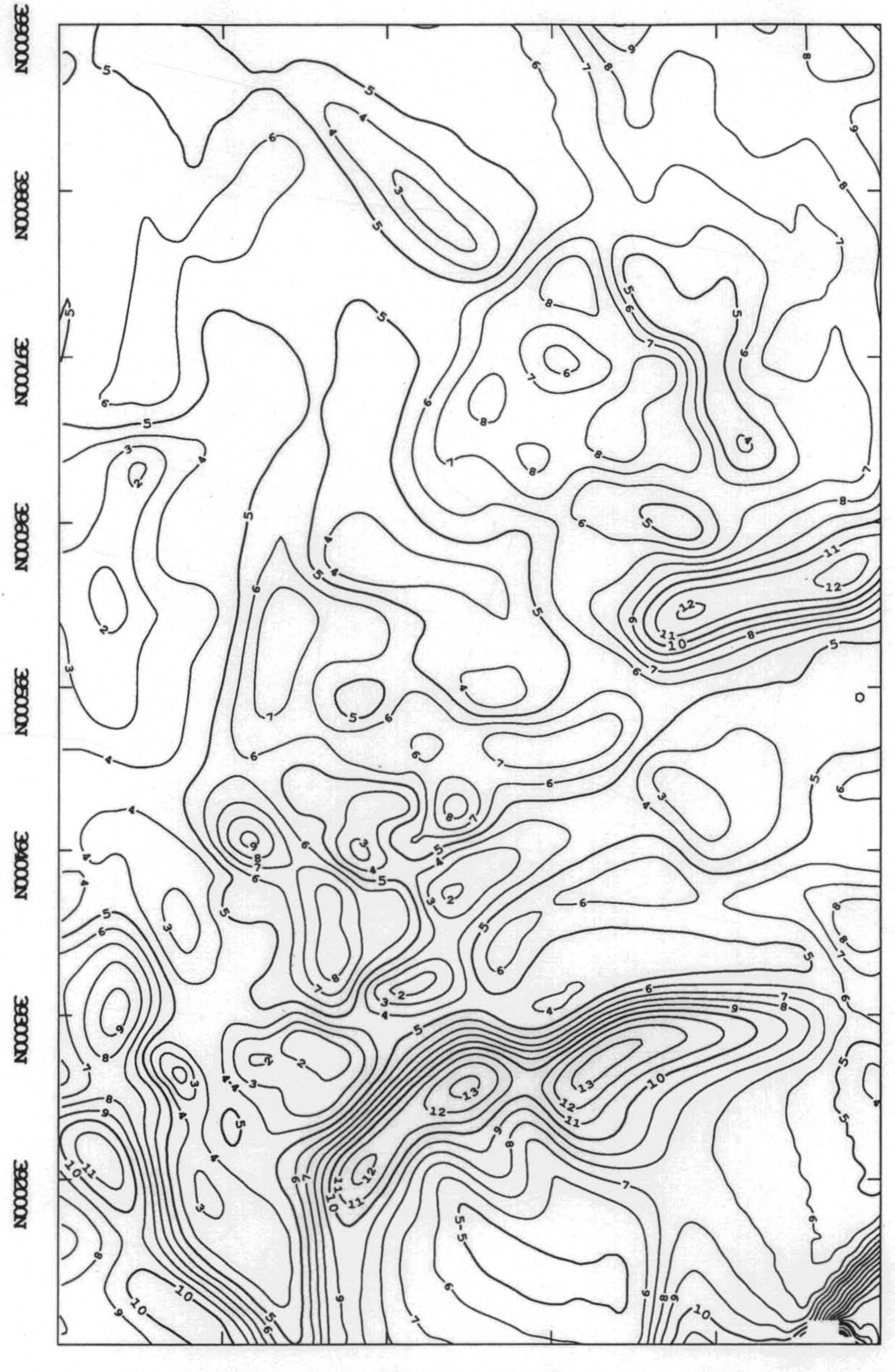

Figure 8

3-D analytic signal of filtered Bouguer Anomaly, Que–Hellyer Area

5 cm

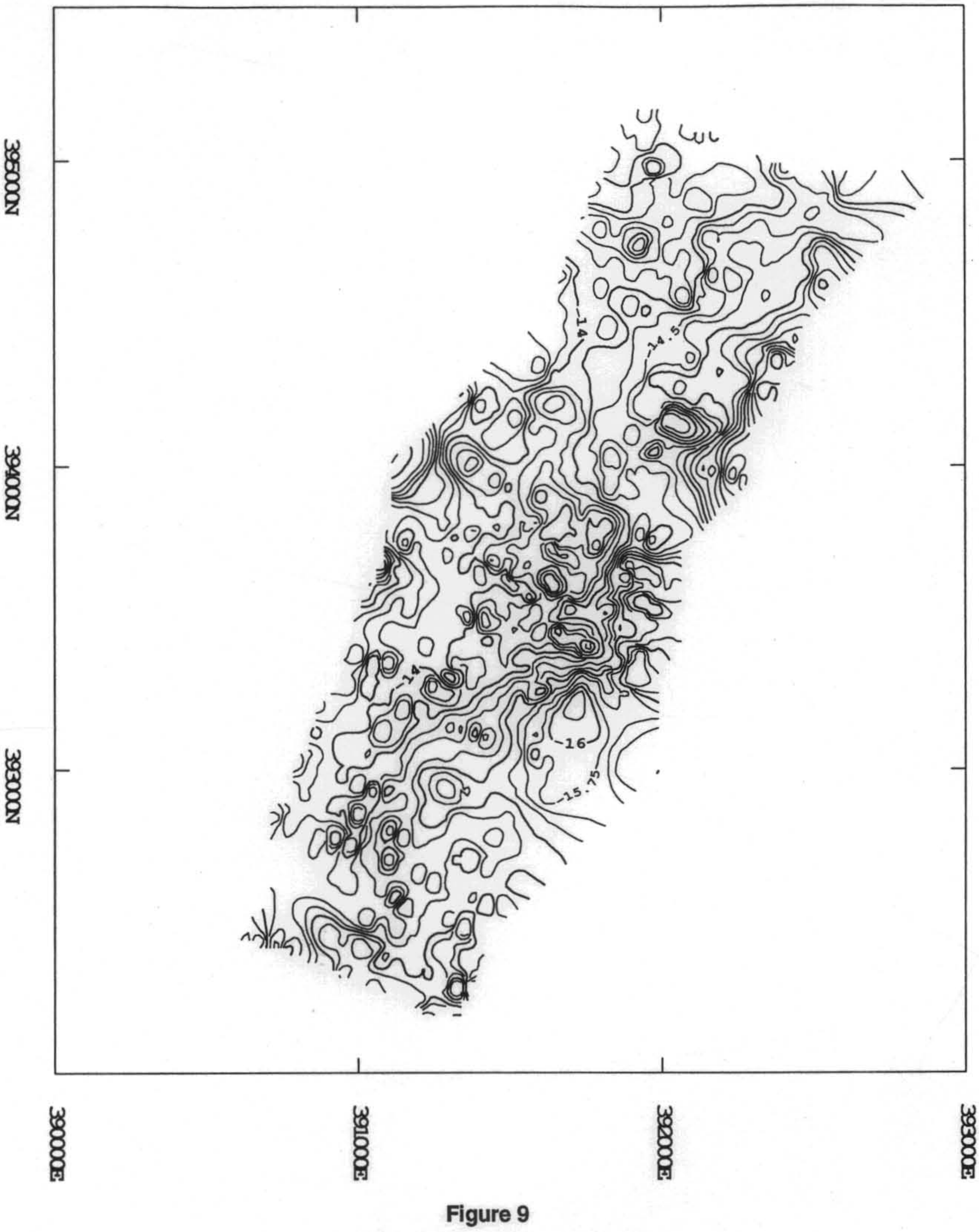

Figure 9

Raw Bouguer Anomaly, Que River

5 cm

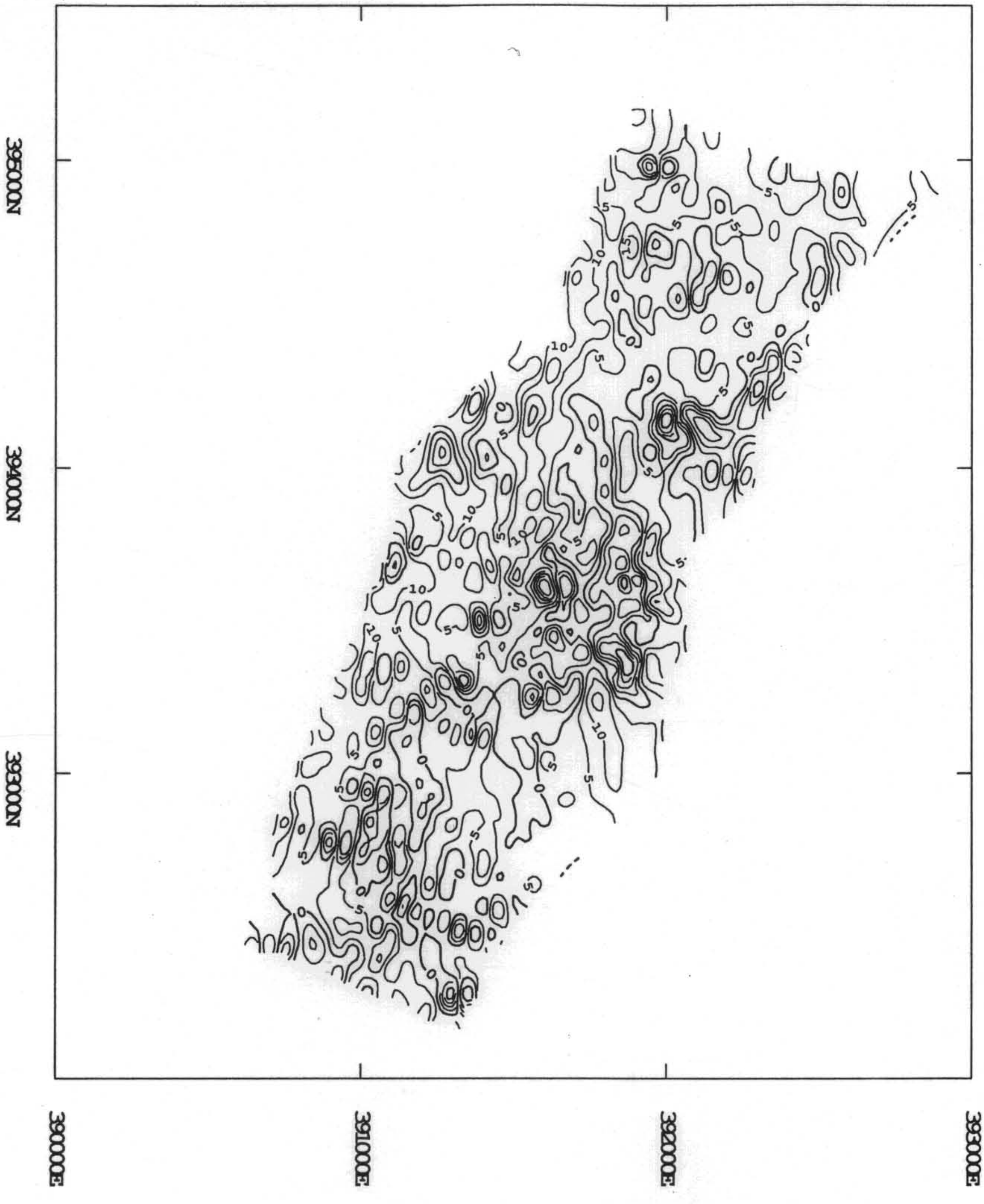

Figure 10

East-west gradient of 100 m radius filtered Bouguer Anomaly, Que River

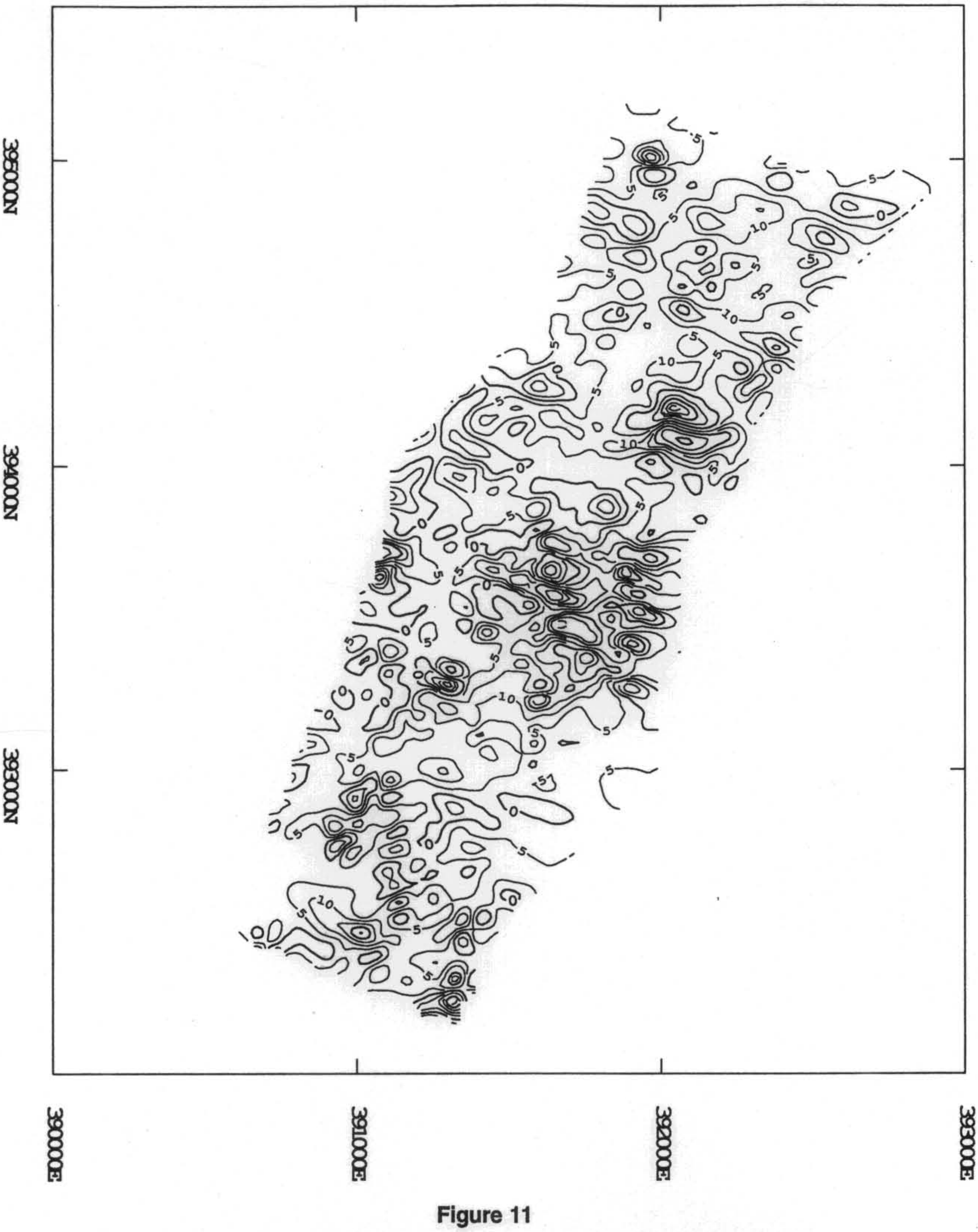

Figure 11

North-south gradient of 100 m radius filtered Bouguer Anomaly, Que River

5 cm

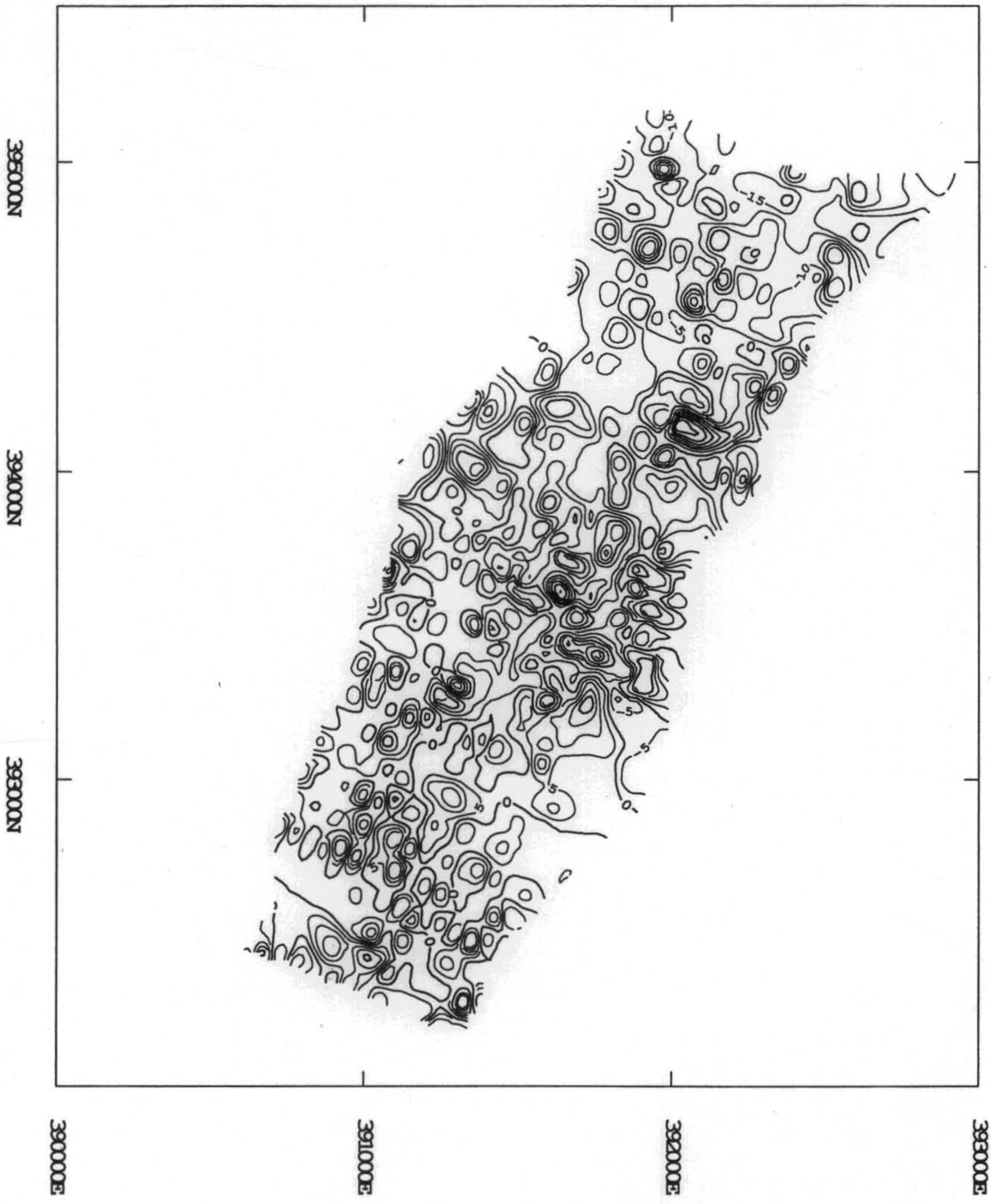

Figure 12
Vertical gradient of 100 m radius filtered Bouguer Anomaly, Que River

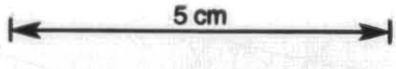

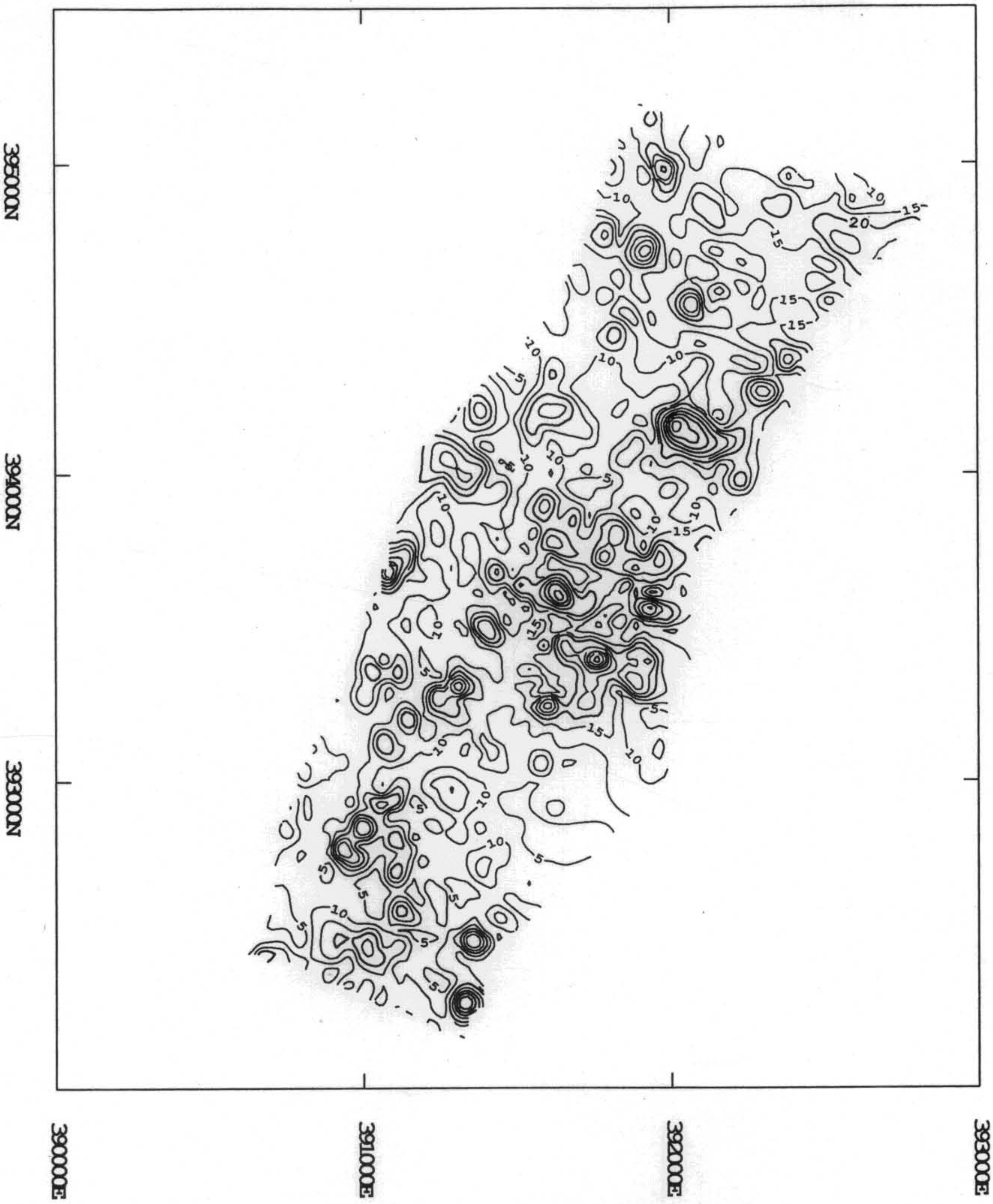

Figure 13

3-D analytic signal of 100 m radius filtered Bouguer Anomaly, Que River

5 cm

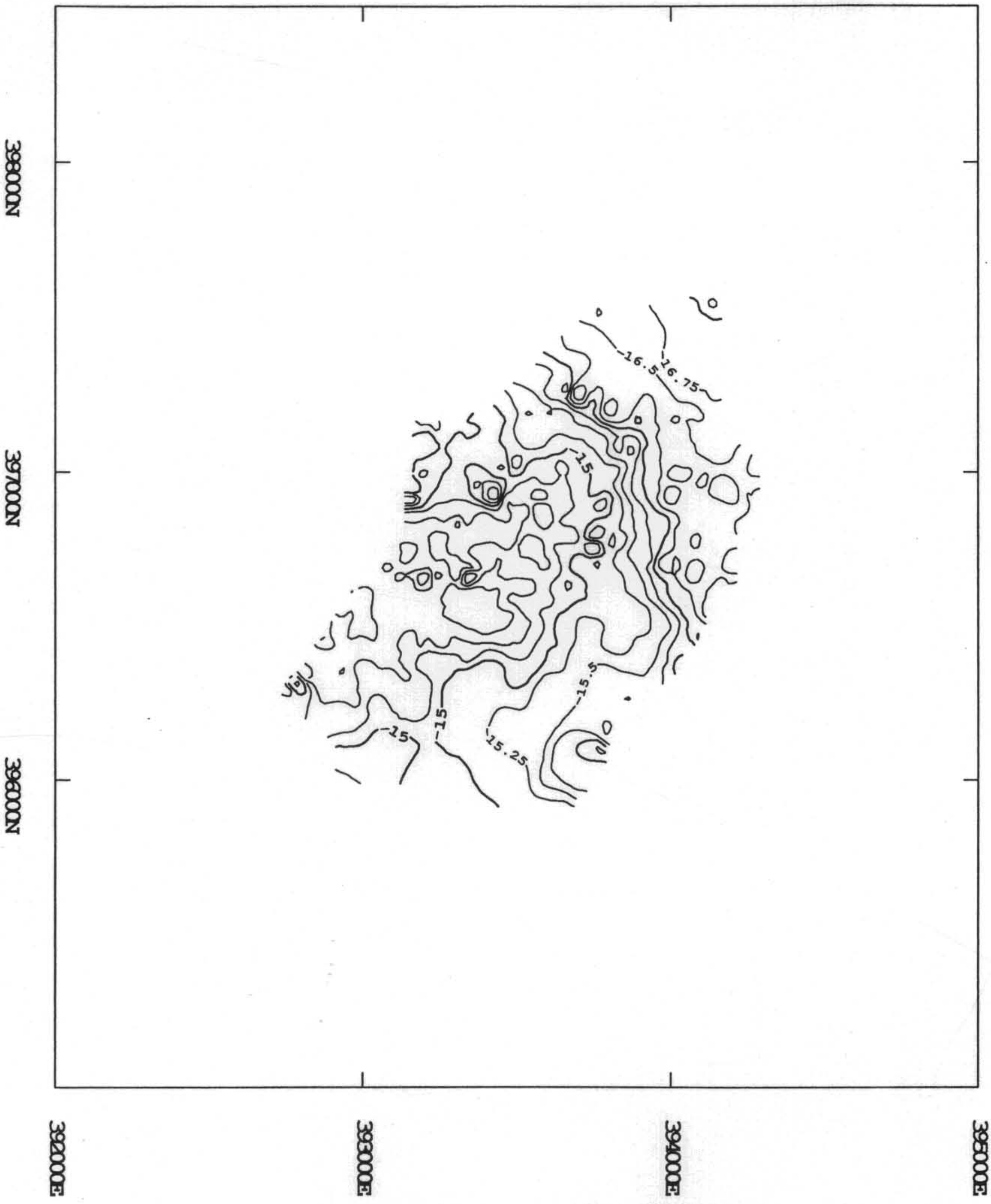

Figure 14
Raw Bouguer Anomaly, Hellyer

5 cm

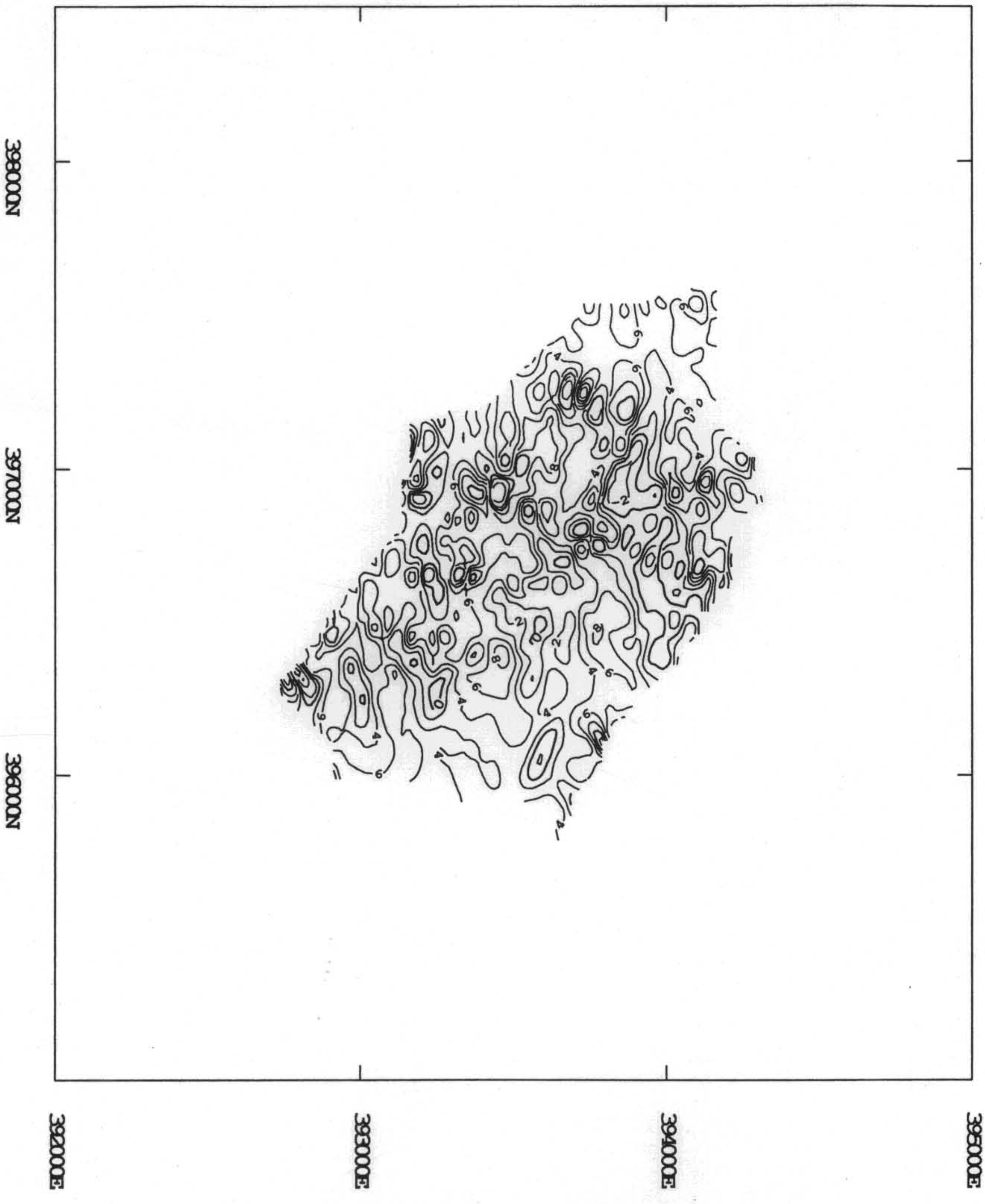

Figure 15

East-west gradient of 100 m radius filtered Bouguer Anomaly, Hellyer

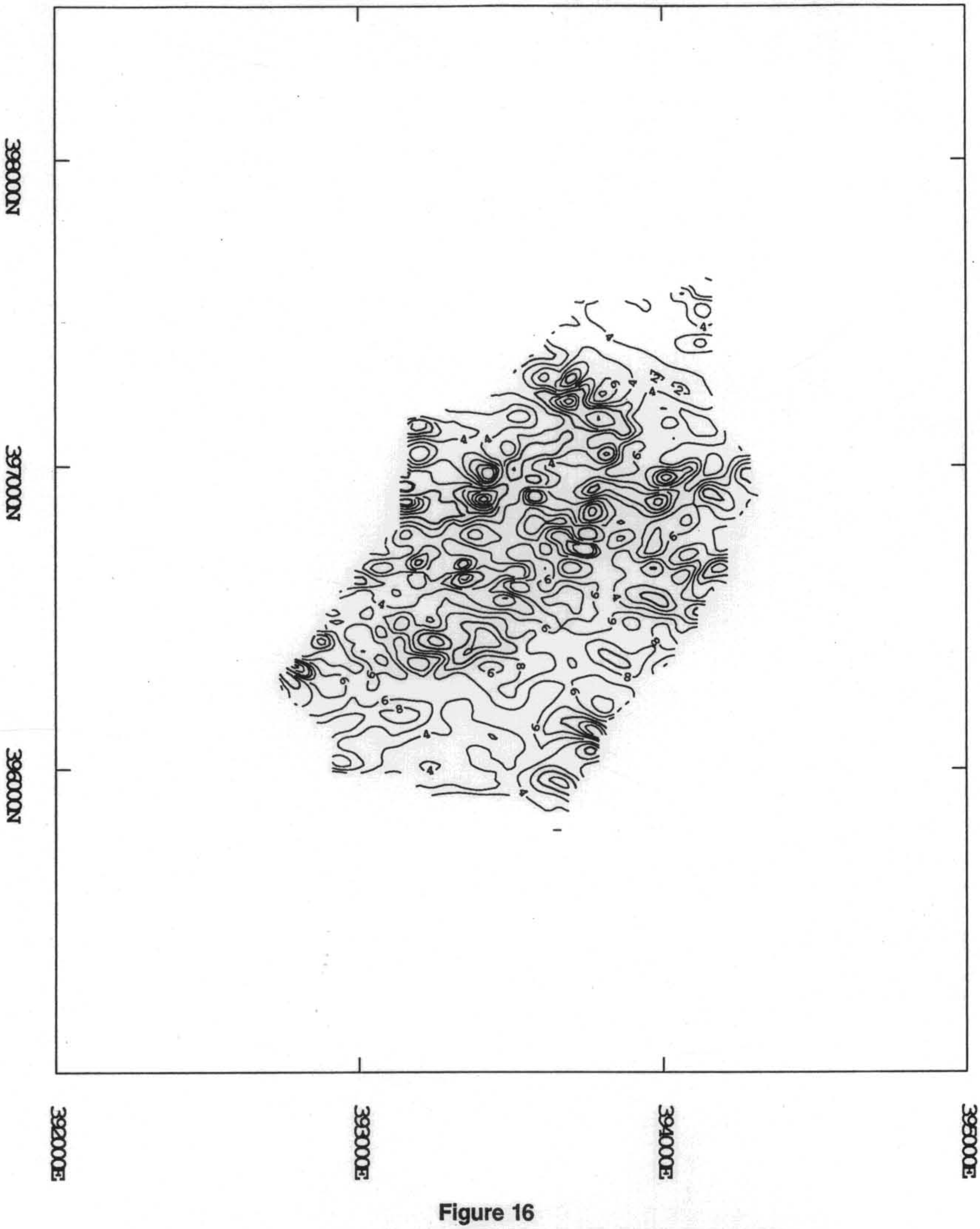

Figure 16
North-south gradient of 100 m radius filtered Bouguer Anomaly, Hellyer

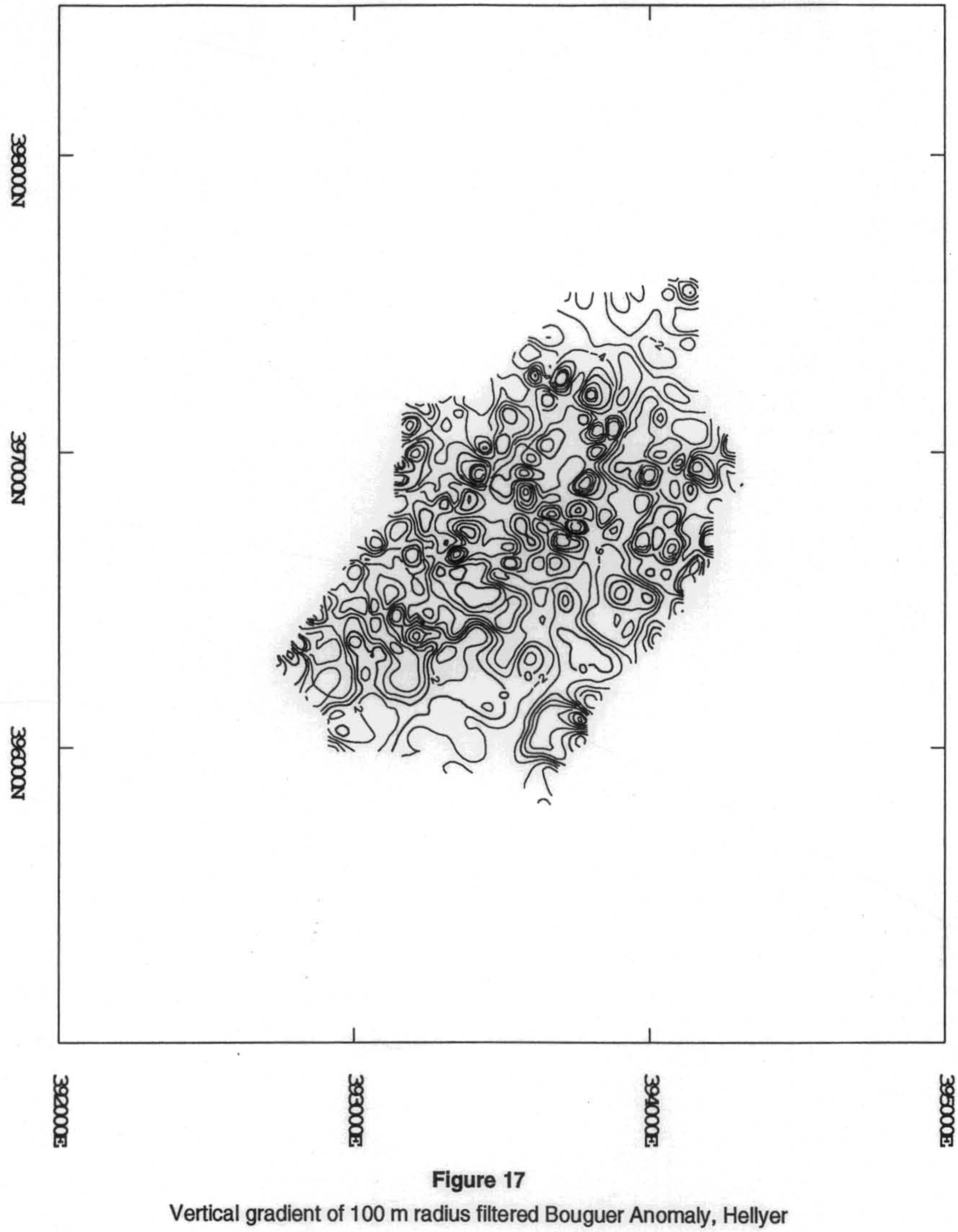

Figure 17
Vertical gradient of 100 m radius filtered Bouguer Anomaly, Hellyer

5 cm

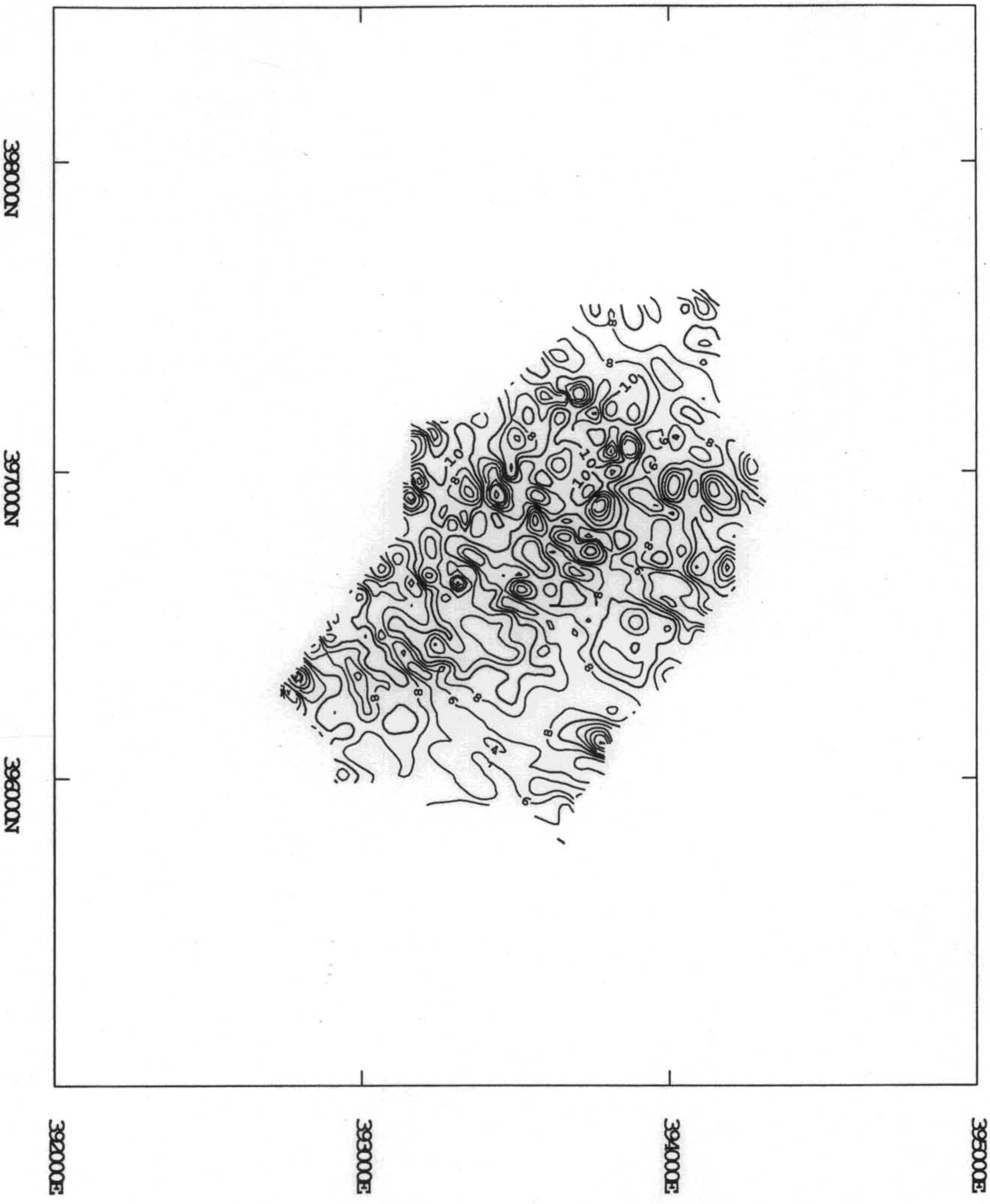

Figure 18

3-D analytic signal of 100 m radius filtered Bouguer Anomaly, Hellyer

5 cm

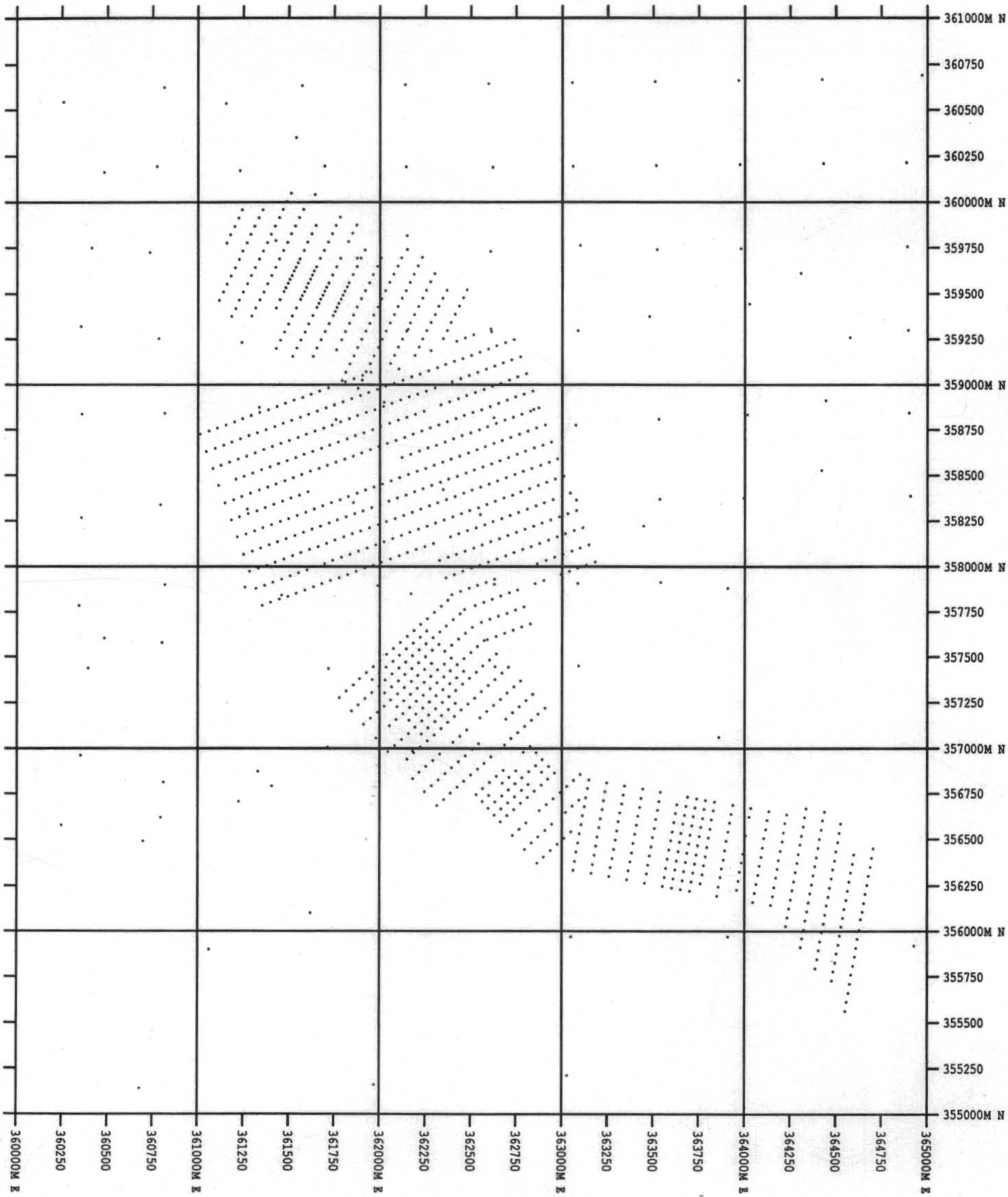

Figure 19
Gravity station distribution, Oceana Area

5 cm

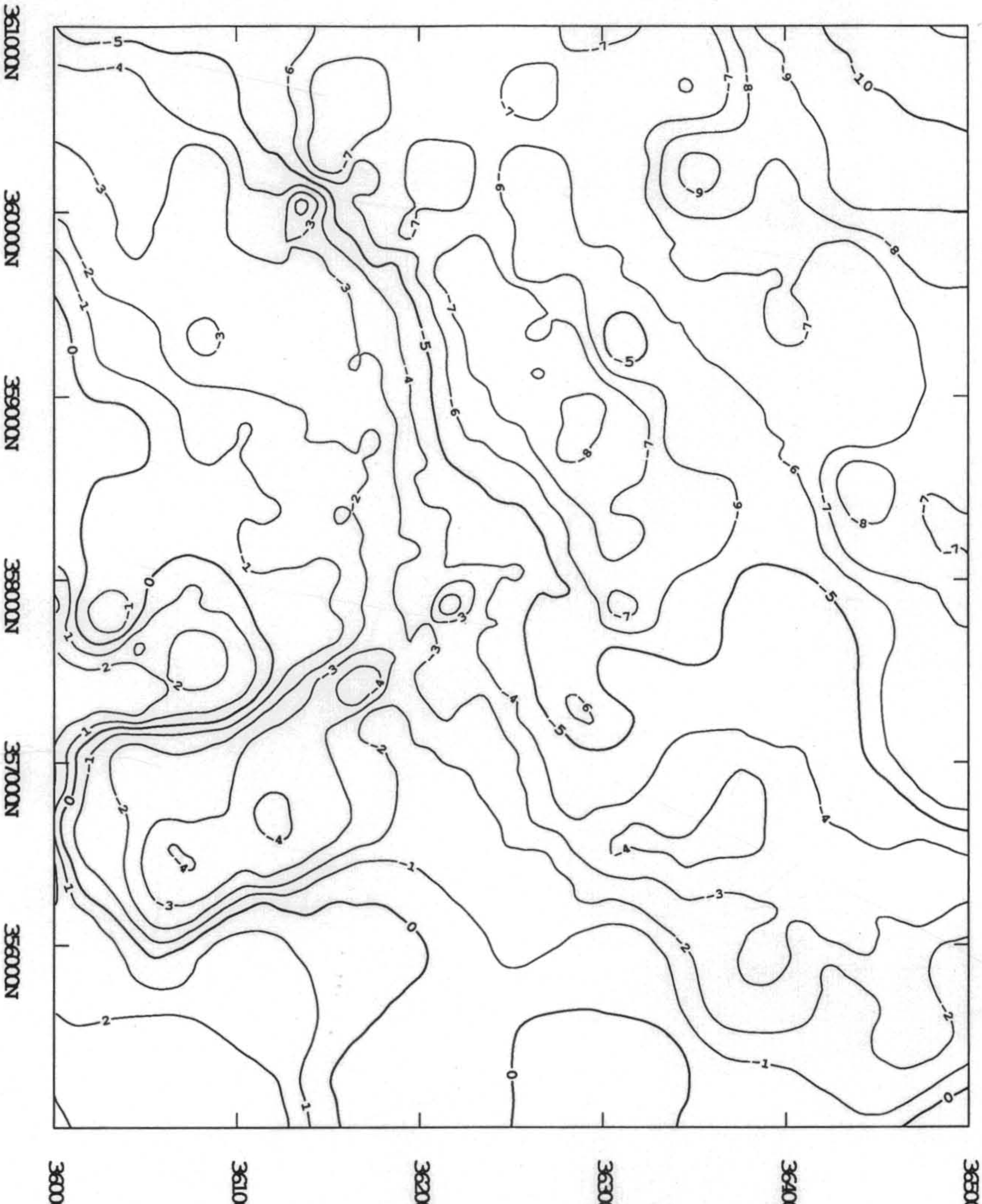

Figure 20
Raw Bouguer Anomaly, Oceana General Area

5 cm

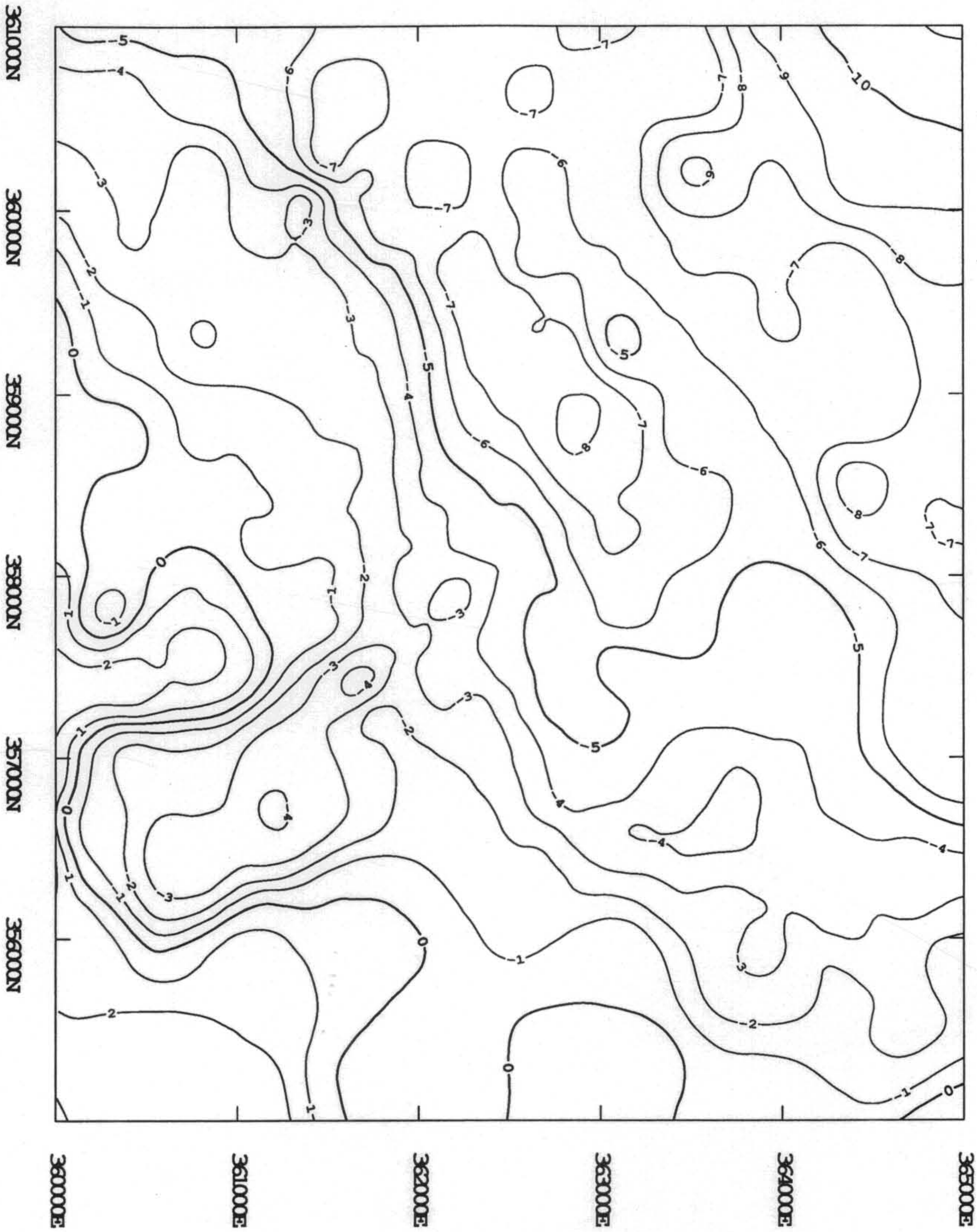

Figure 21

Bouguer Anomaly filtered 300 m radius, Oceana General Area

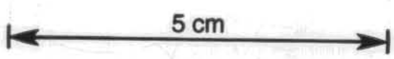

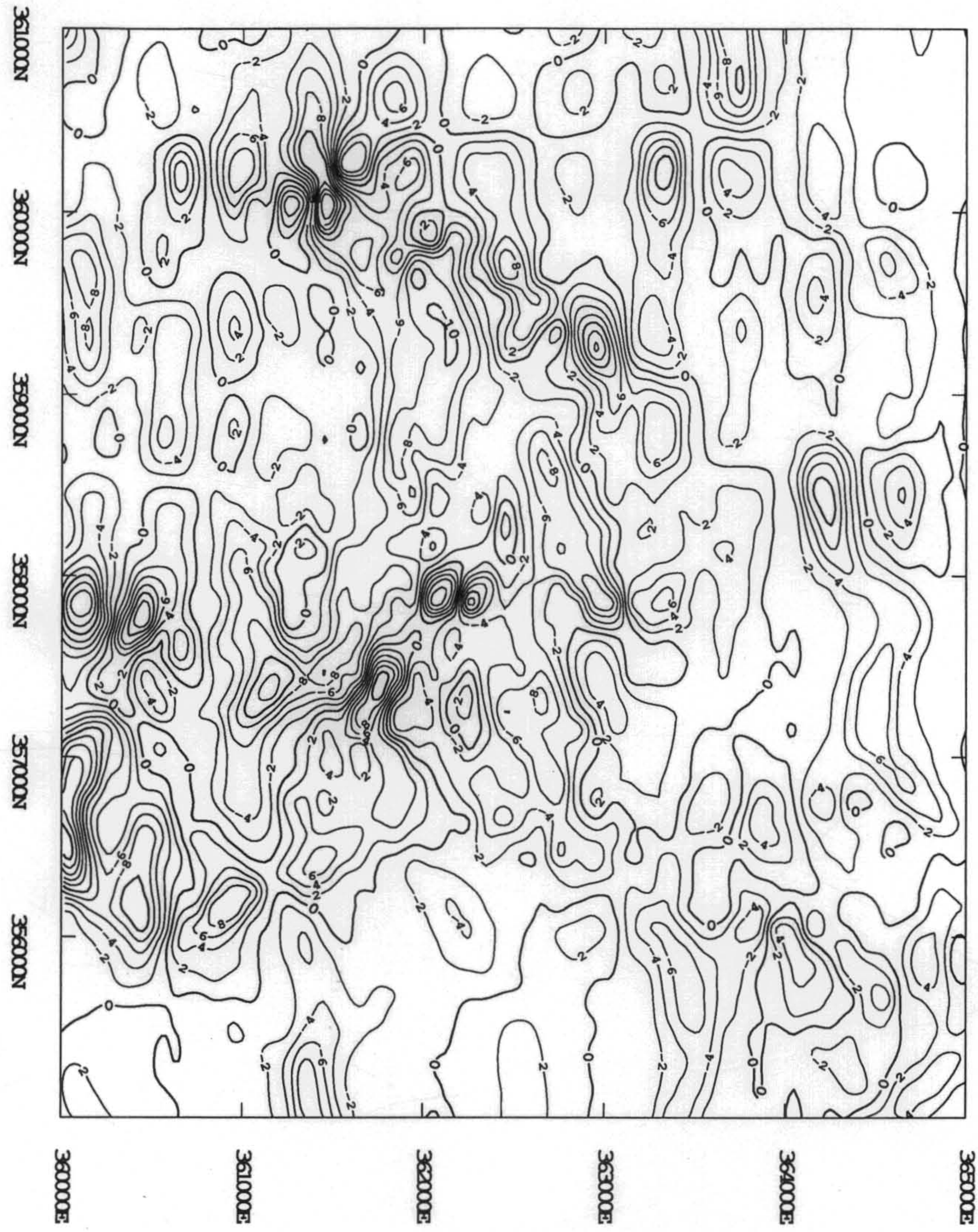

Figure 22

East-west gradient of 300 m radius filtered Bouguer Anomaly, Oceana General Area

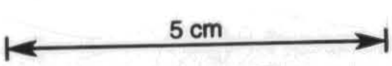

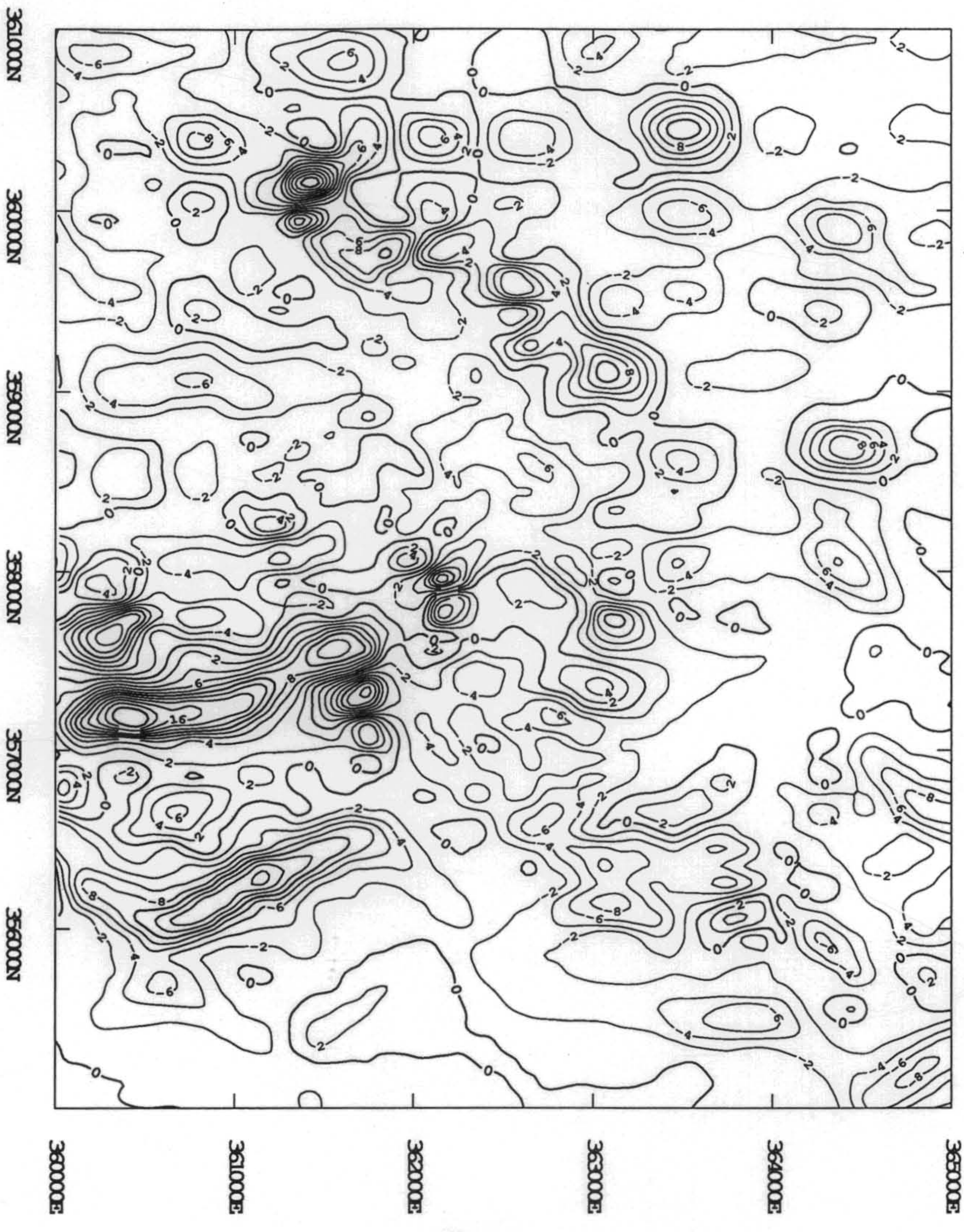

Figure 23

North-south gradient of 300 m radius filtered Bouguer Anomaly, Oceana General Area

5 cm

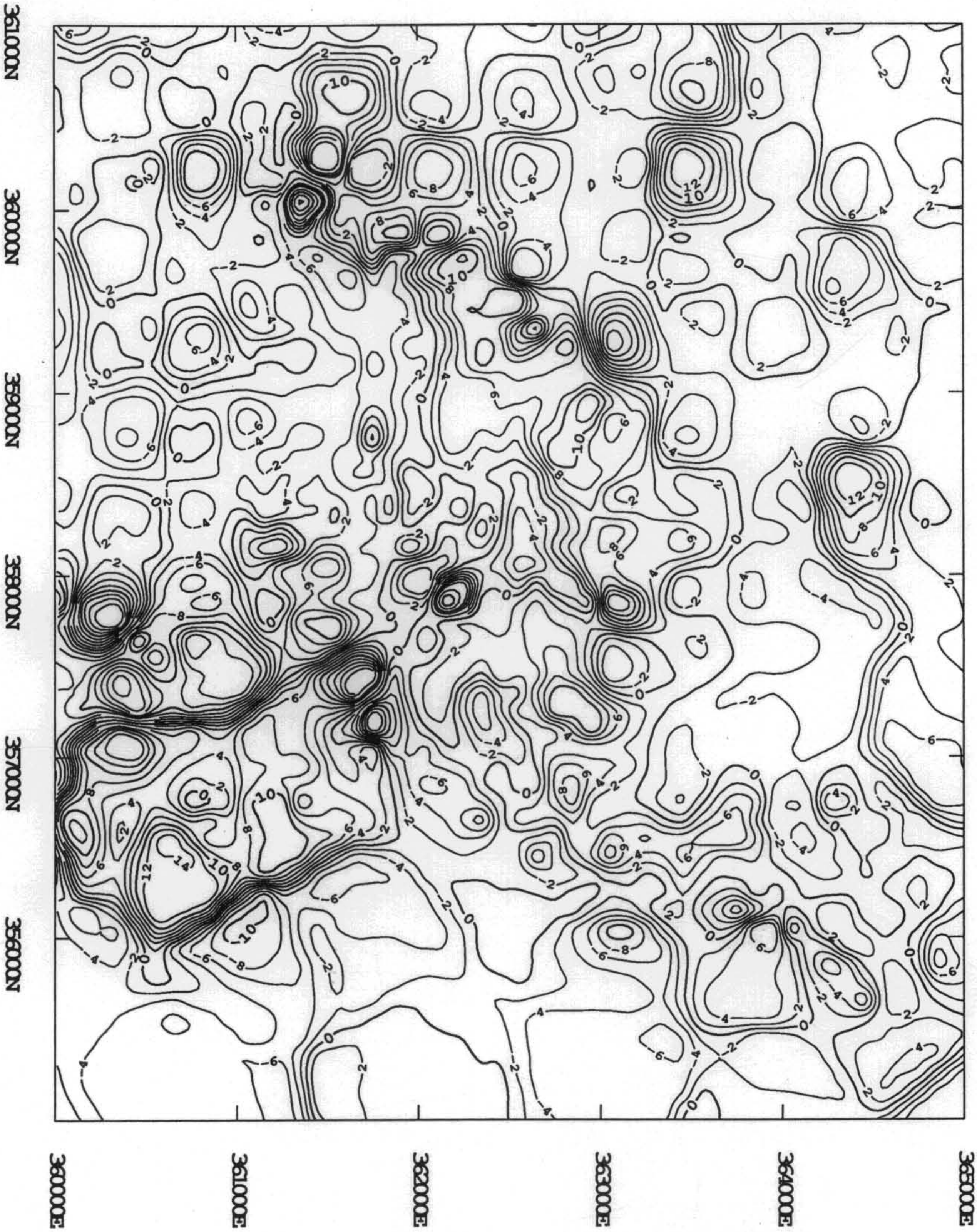

Figure 24

Vertical gradient of 300 m radius filtered Bouguer Anomaly, Oceana General Area

5 cm

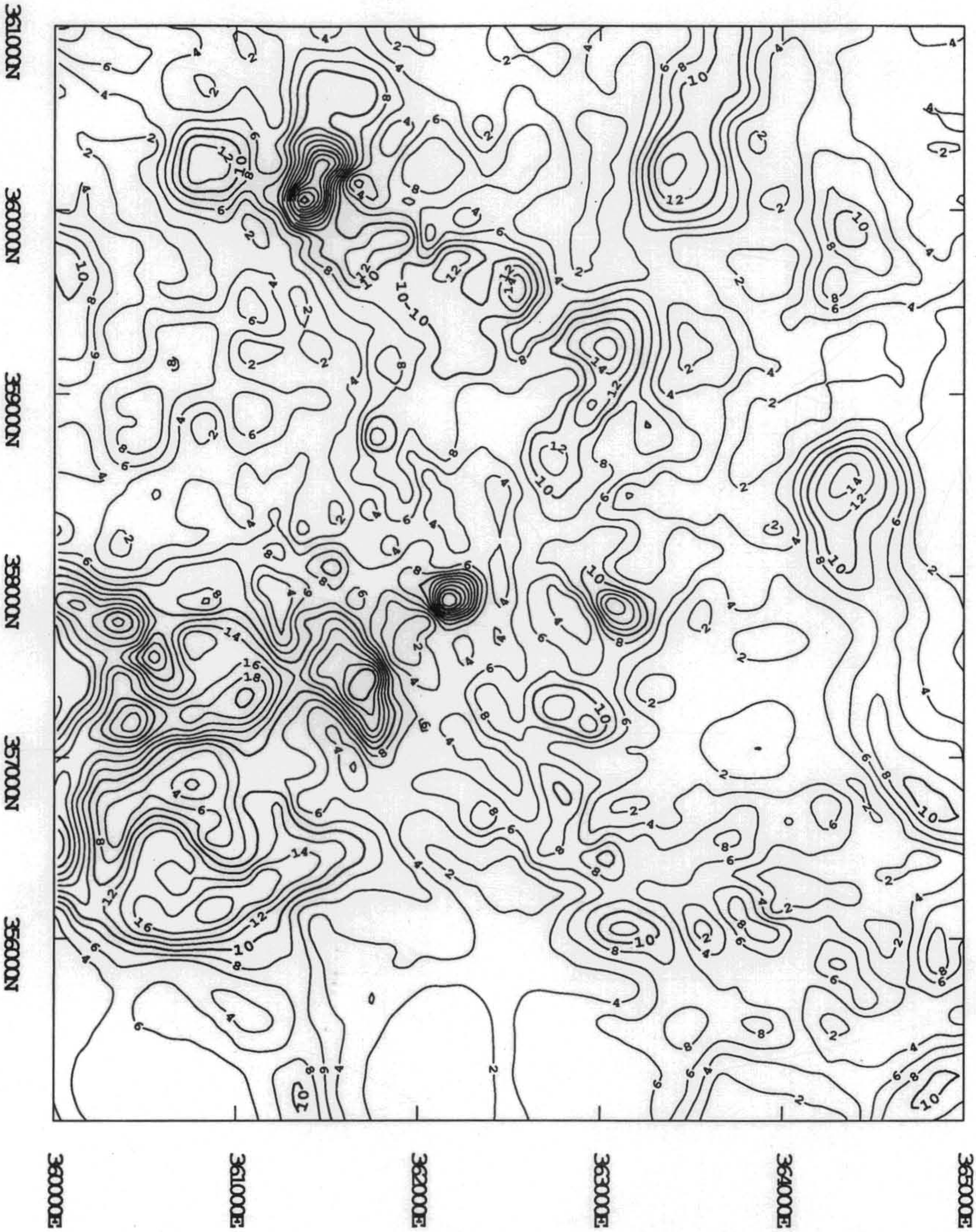

Figure 25

3-D analytic signal of 300 m radius filtered Bouguer Anomaly, Oceana General Area

5 cm

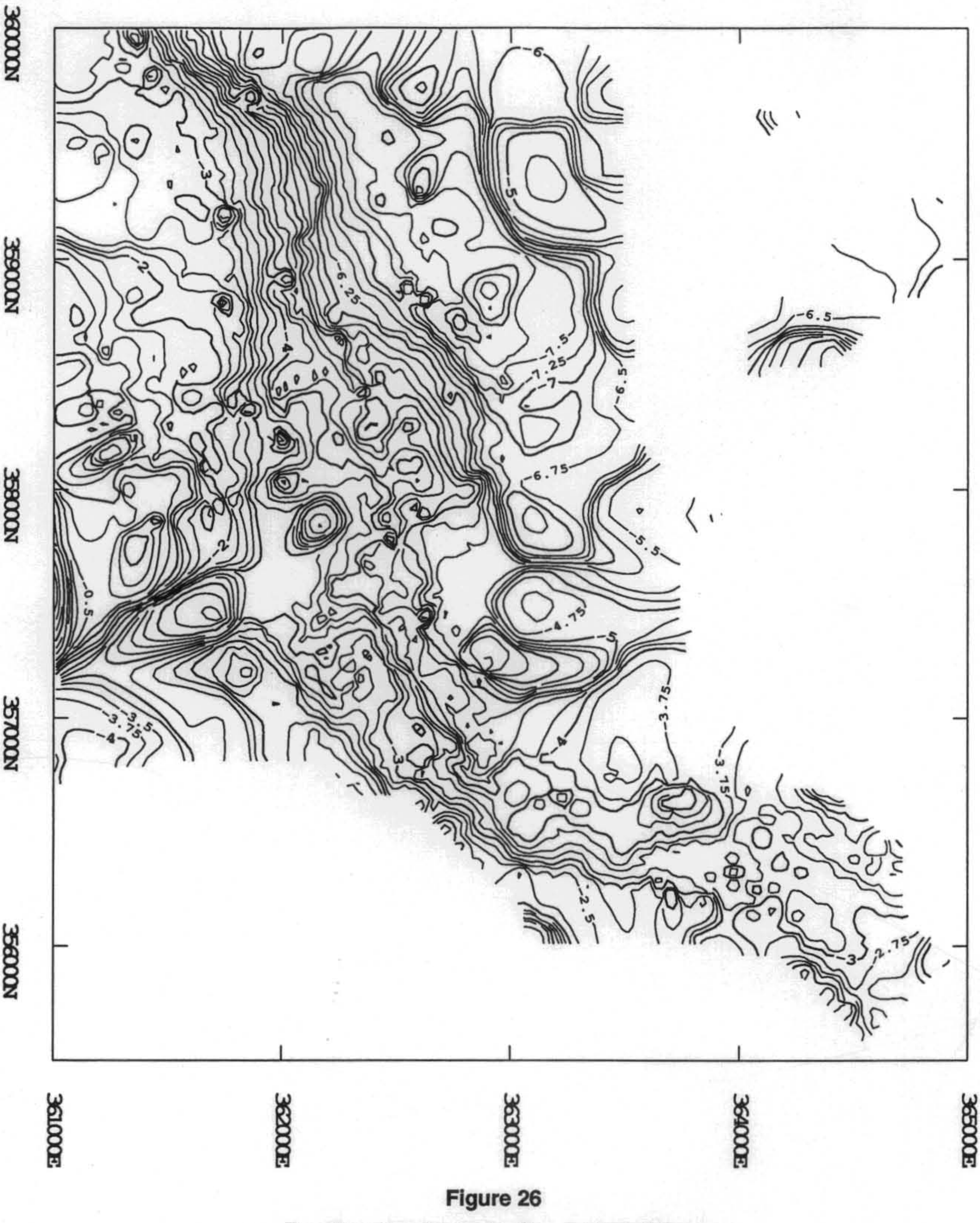

Figure 26
Raw Bouguer Anomaly, Oceana Detail Area

5 cm

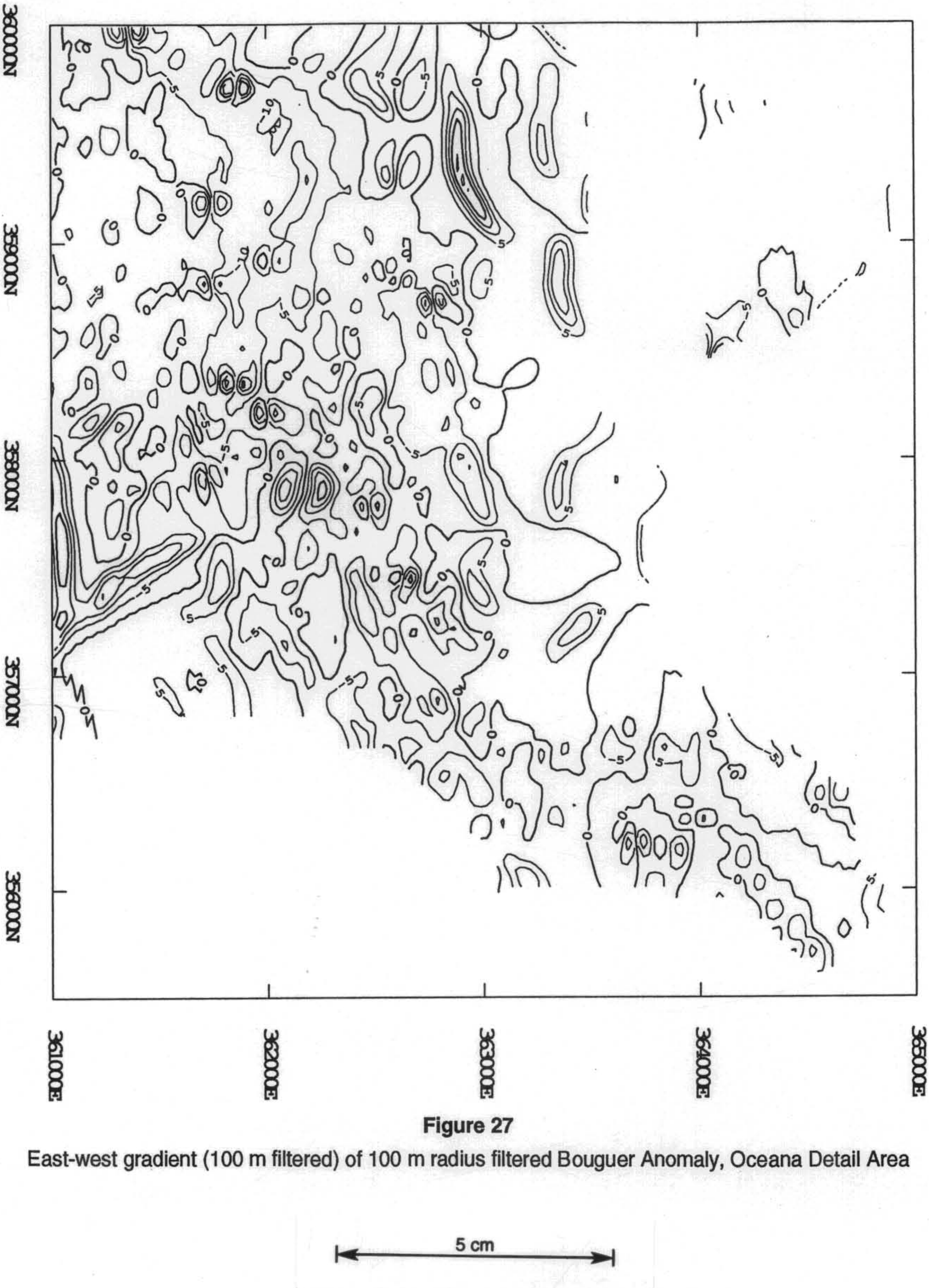

Figure 27

East-west gradient (100 m filtered) of 100 m radius filtered Bouguer Anomaly, Oceana Detail Area

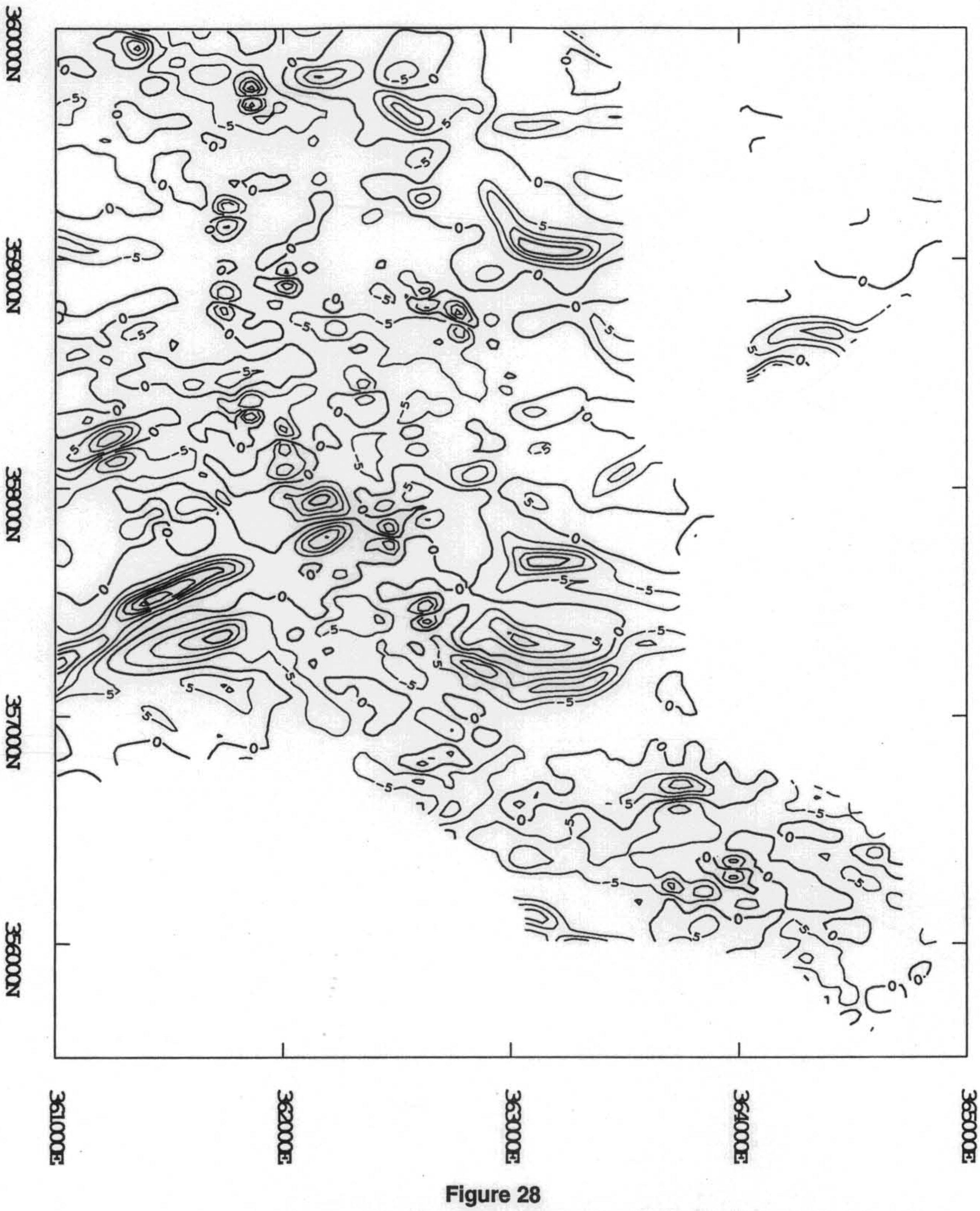

Figure 28

North-south gradient (100 m filtered) of 100 m radius filtered Bouguer Anomaly, Oceana Detail Area

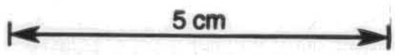

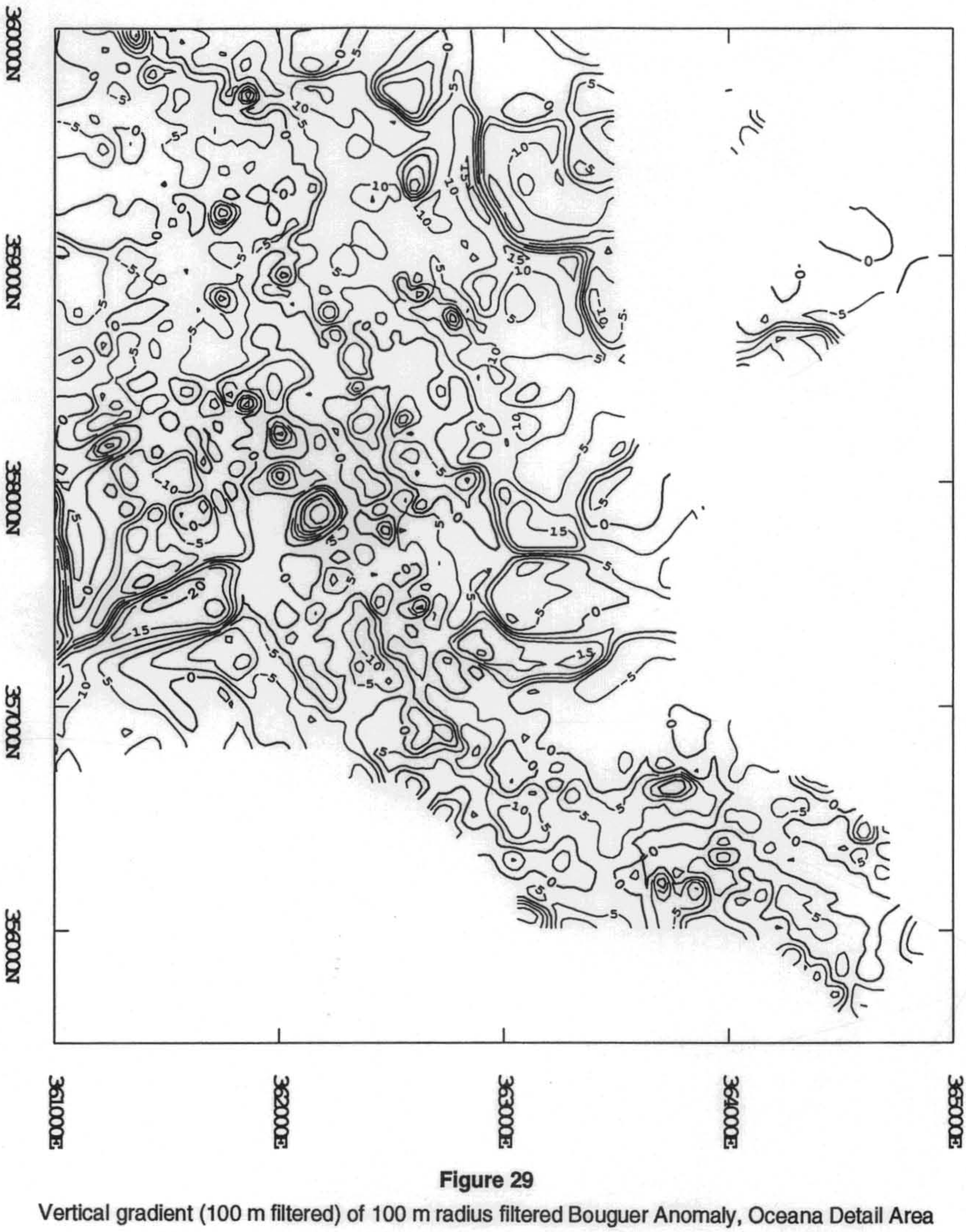

Figure 29

Vertical gradient (100 m filtered) of 100 m radius filtered Bouguer Anomaly, Oceana Detail Area

5 cm

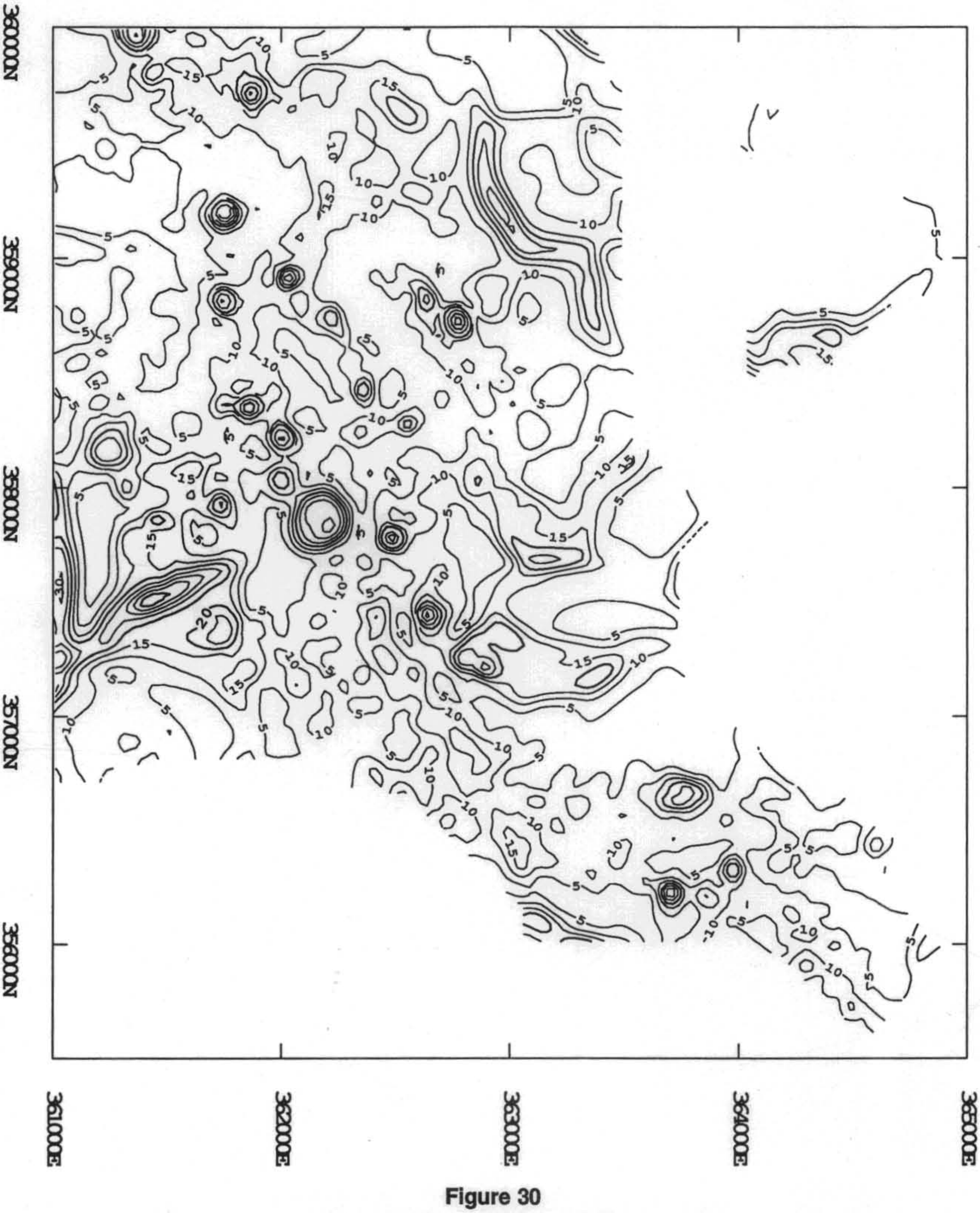

Figure 30

3-D analytic signal (100 m filtered) of 100 m radius filtered Bouguer Anomaly, Oceana Detail Area

5 cm

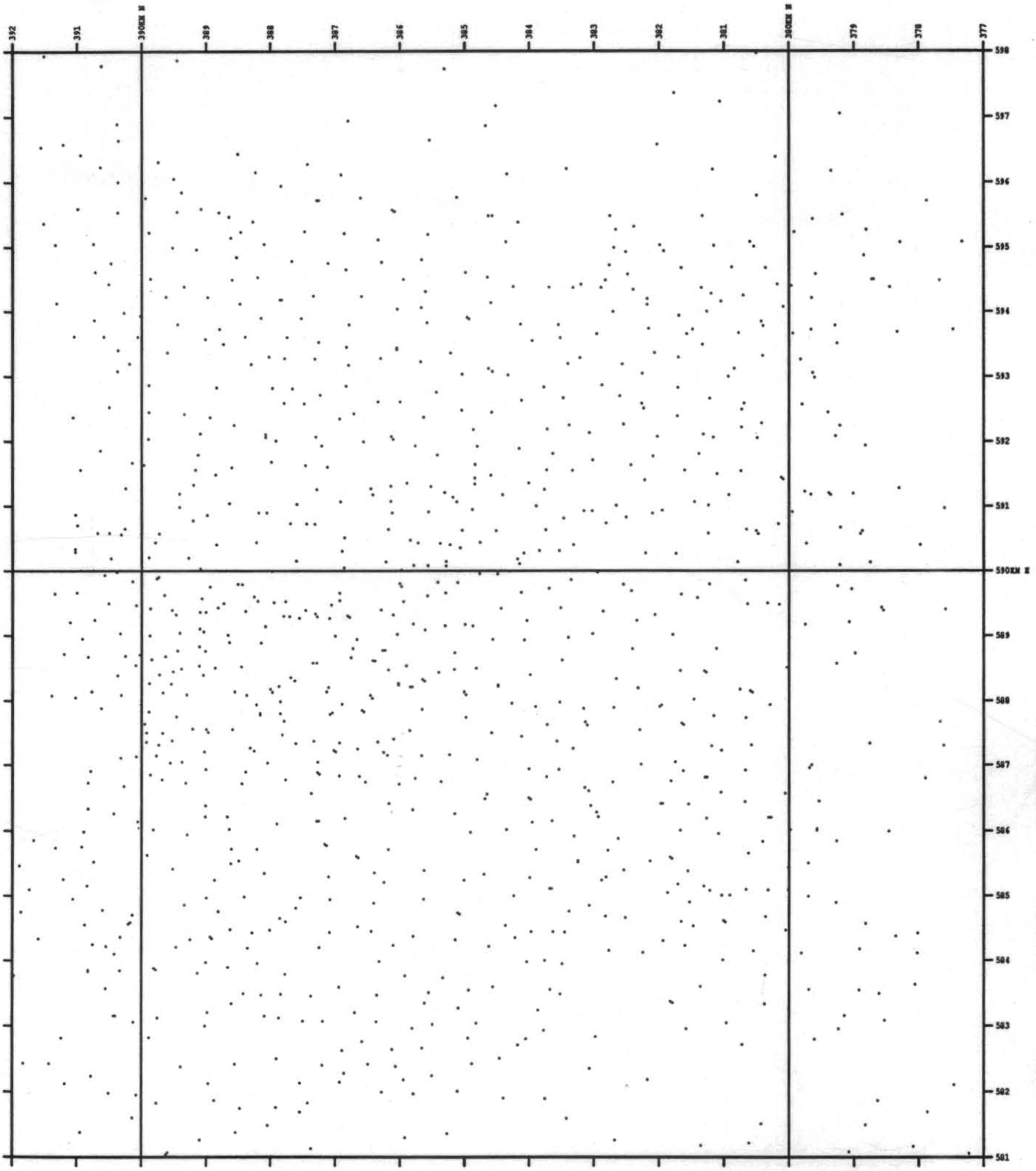

Figure 31
Gravity station distribution, Fingal Tier

5 cm

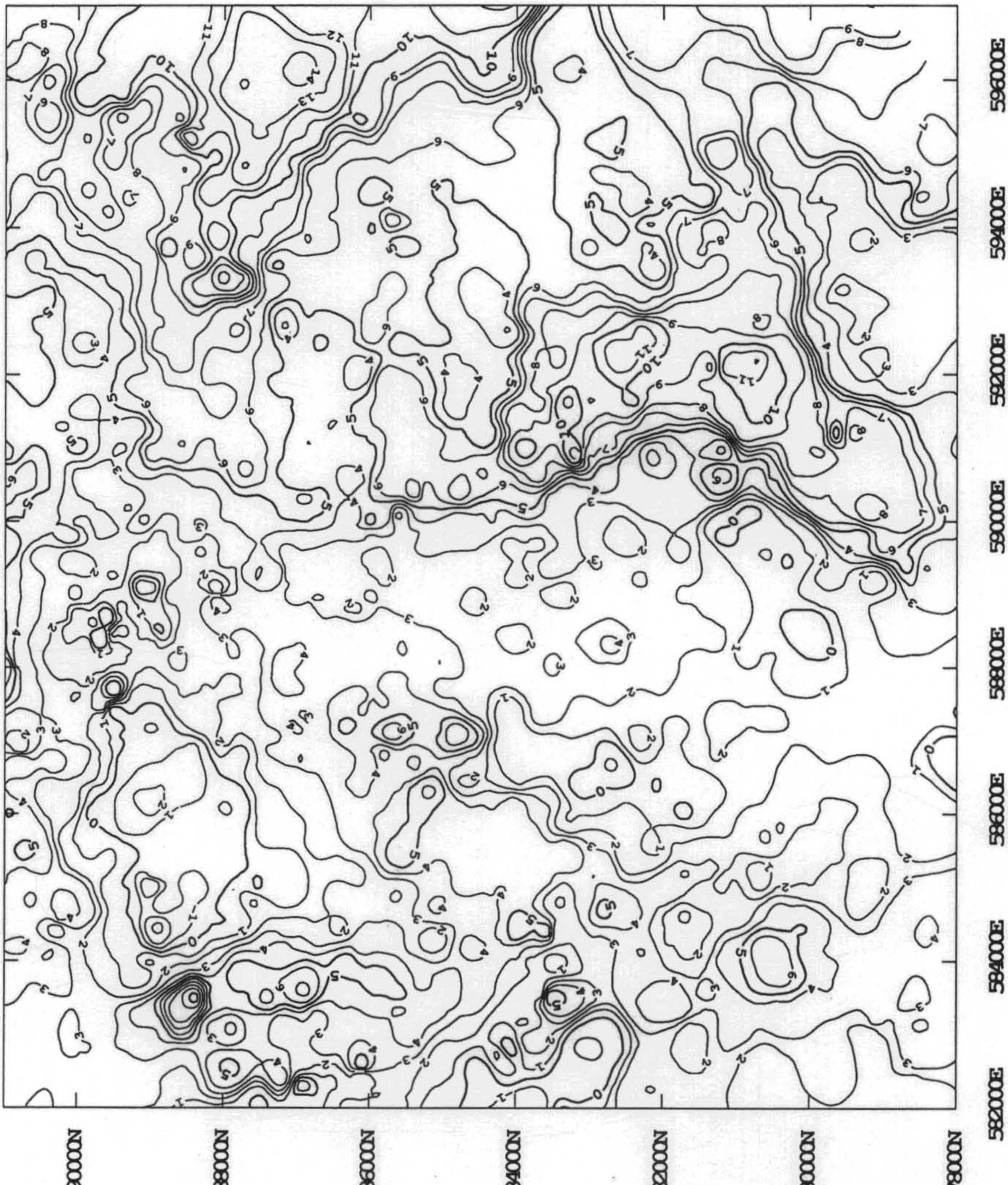

Figure 32
Raw Bouguer Anomaly, Fingal Tier

5 cm

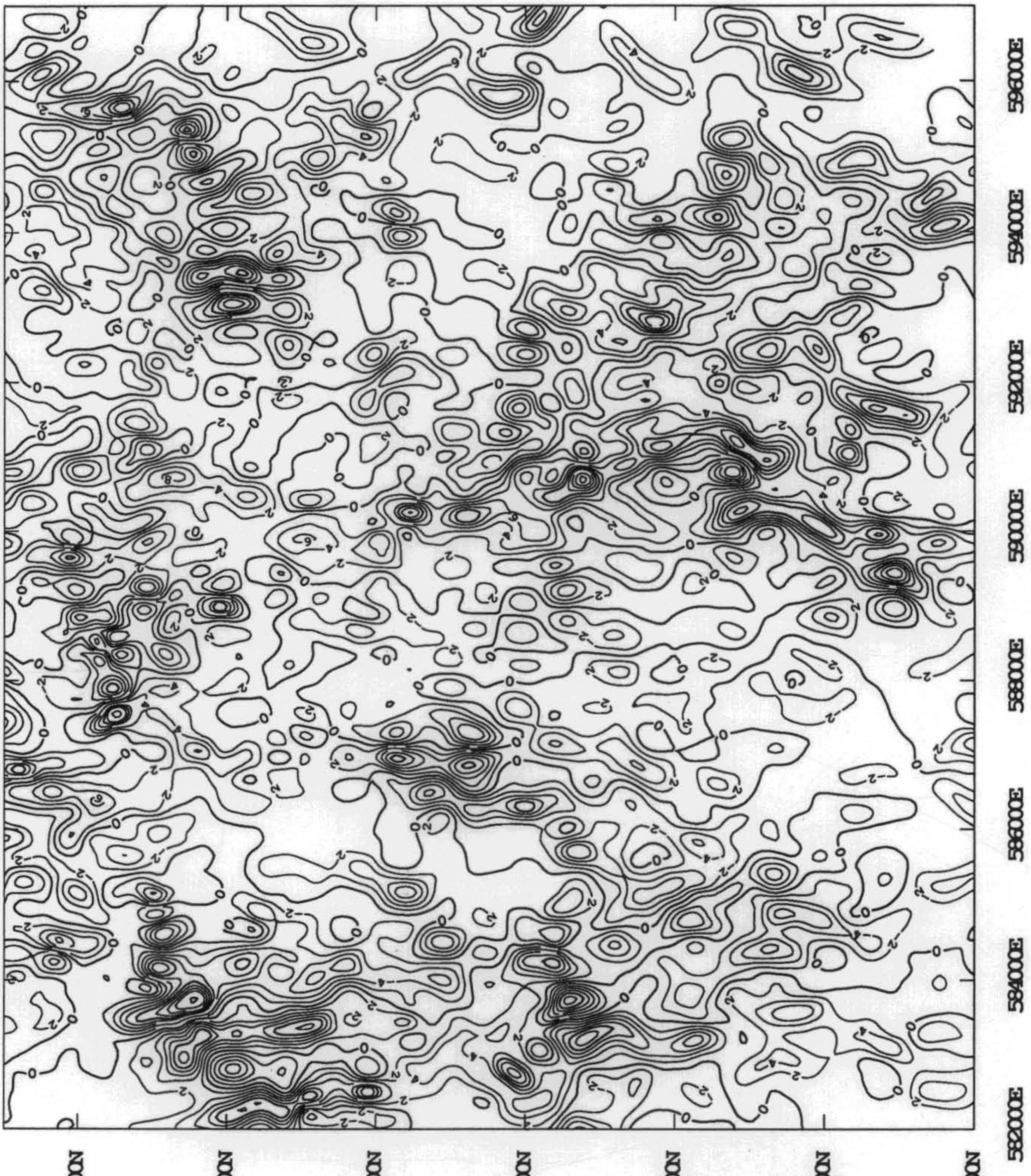

Figure 33

East-west gradient (500 m filtered) of Bouguer Anomaly, Fingal Tier

5 cm

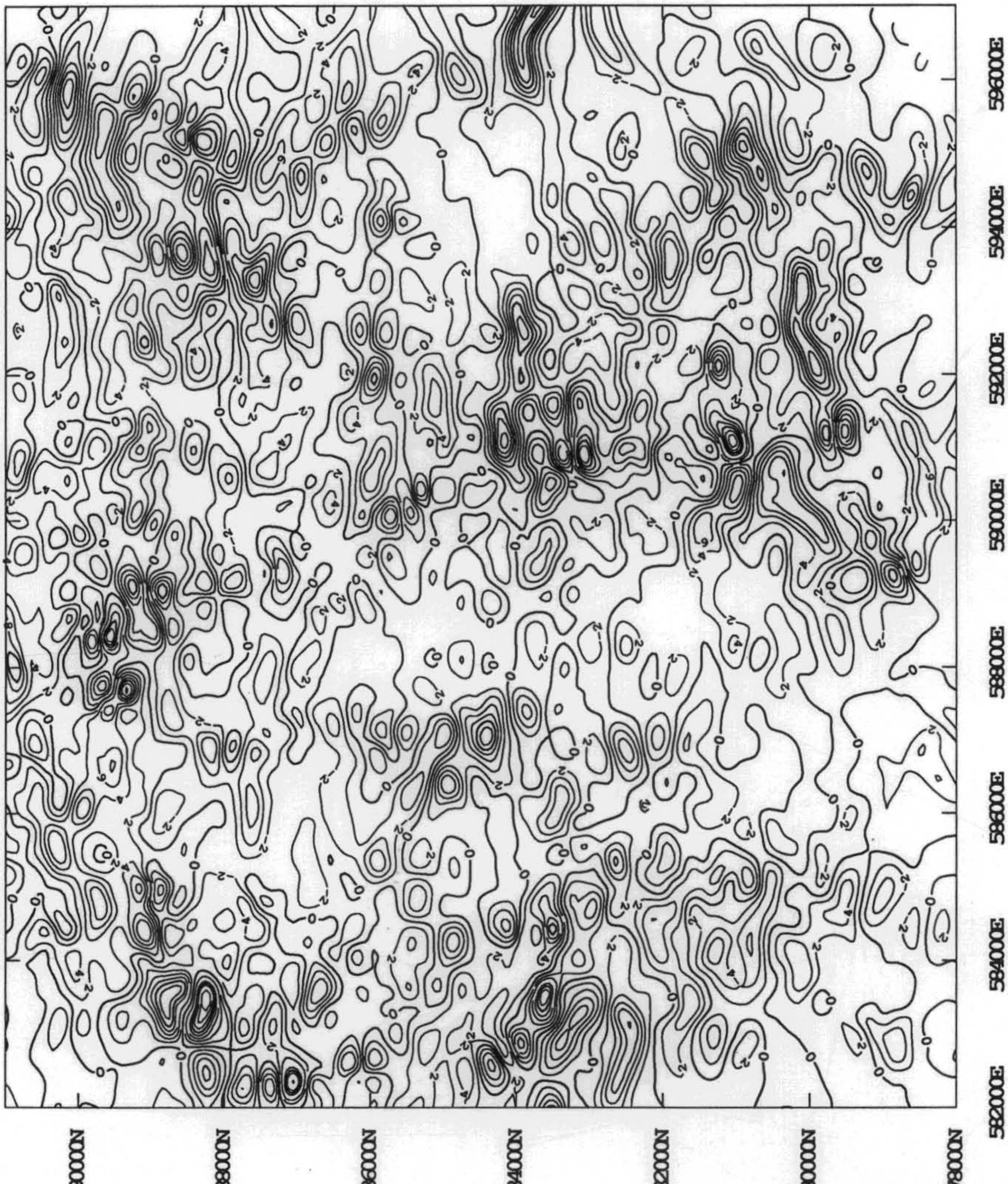

Figure 34

North-south gradient (500 m filtered) of Bouguer Anomaly, Fingal Tier

5 cm

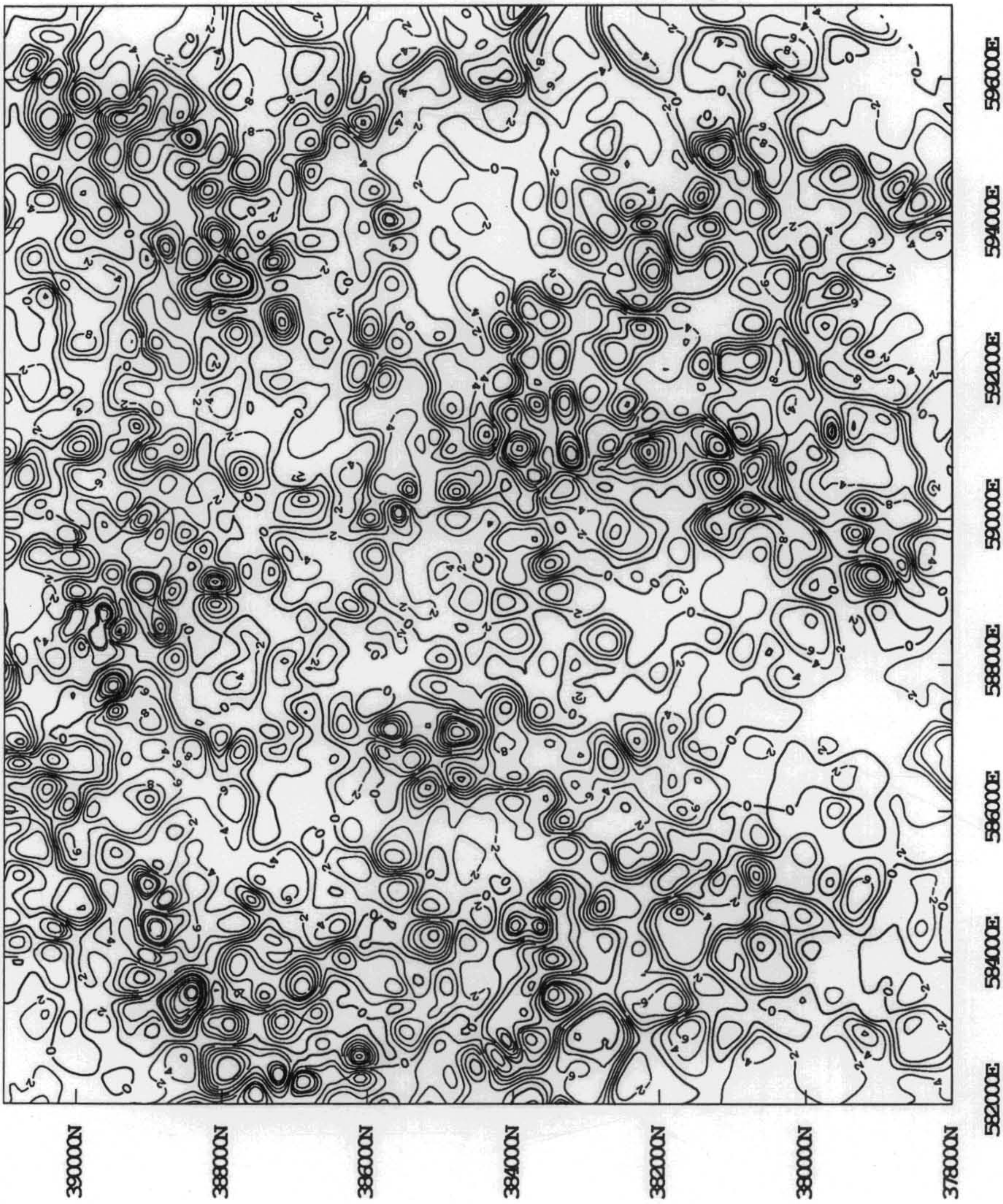

Figure 35
Vertical gradient (500 m filtered) of Bouguer Anomaly, Fingal Tier

5 cm

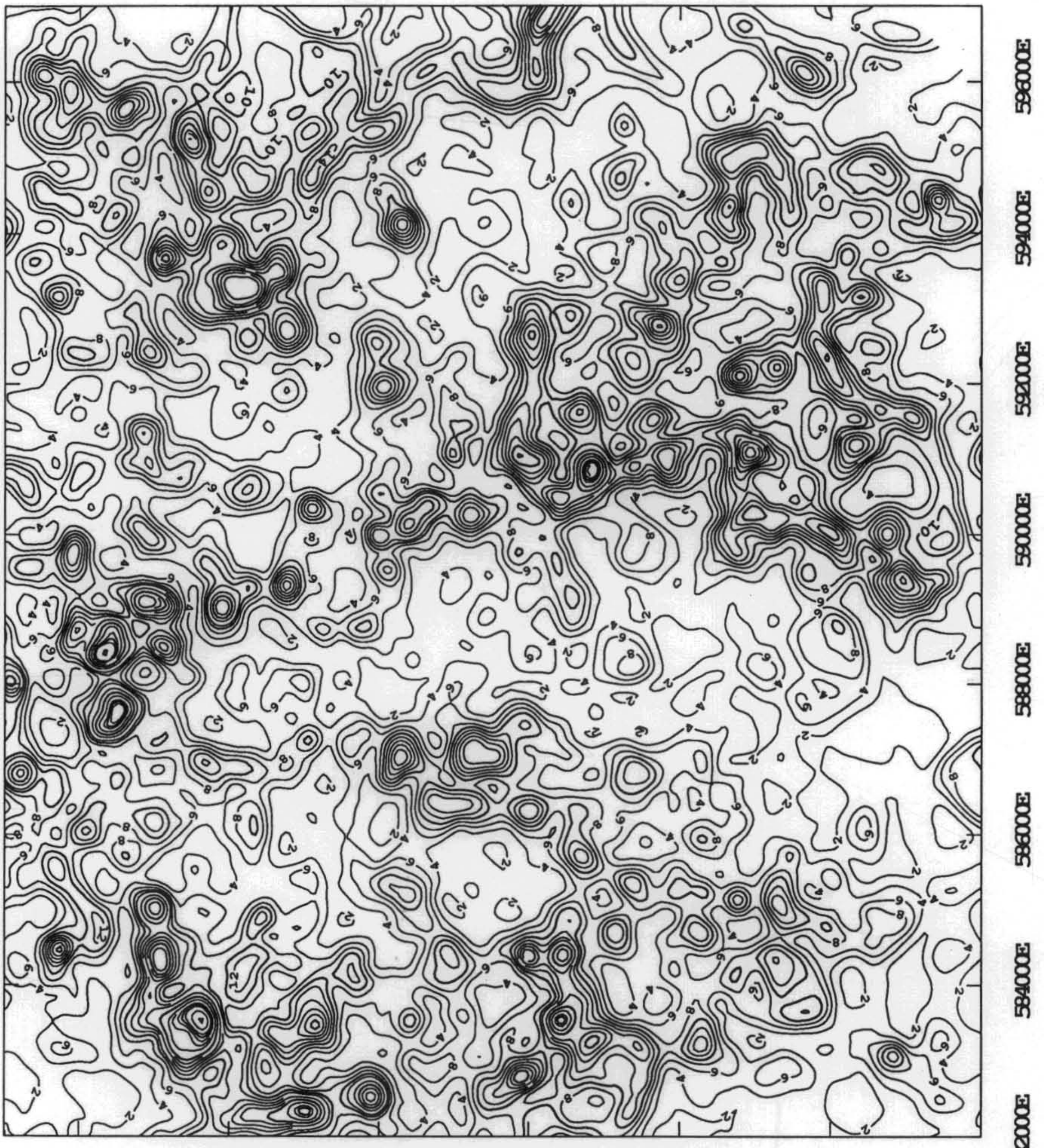

Figure 36

3-D analytic signal (500 m filtered) of Bouguer Anomaly, Fingal Tier

5 cm

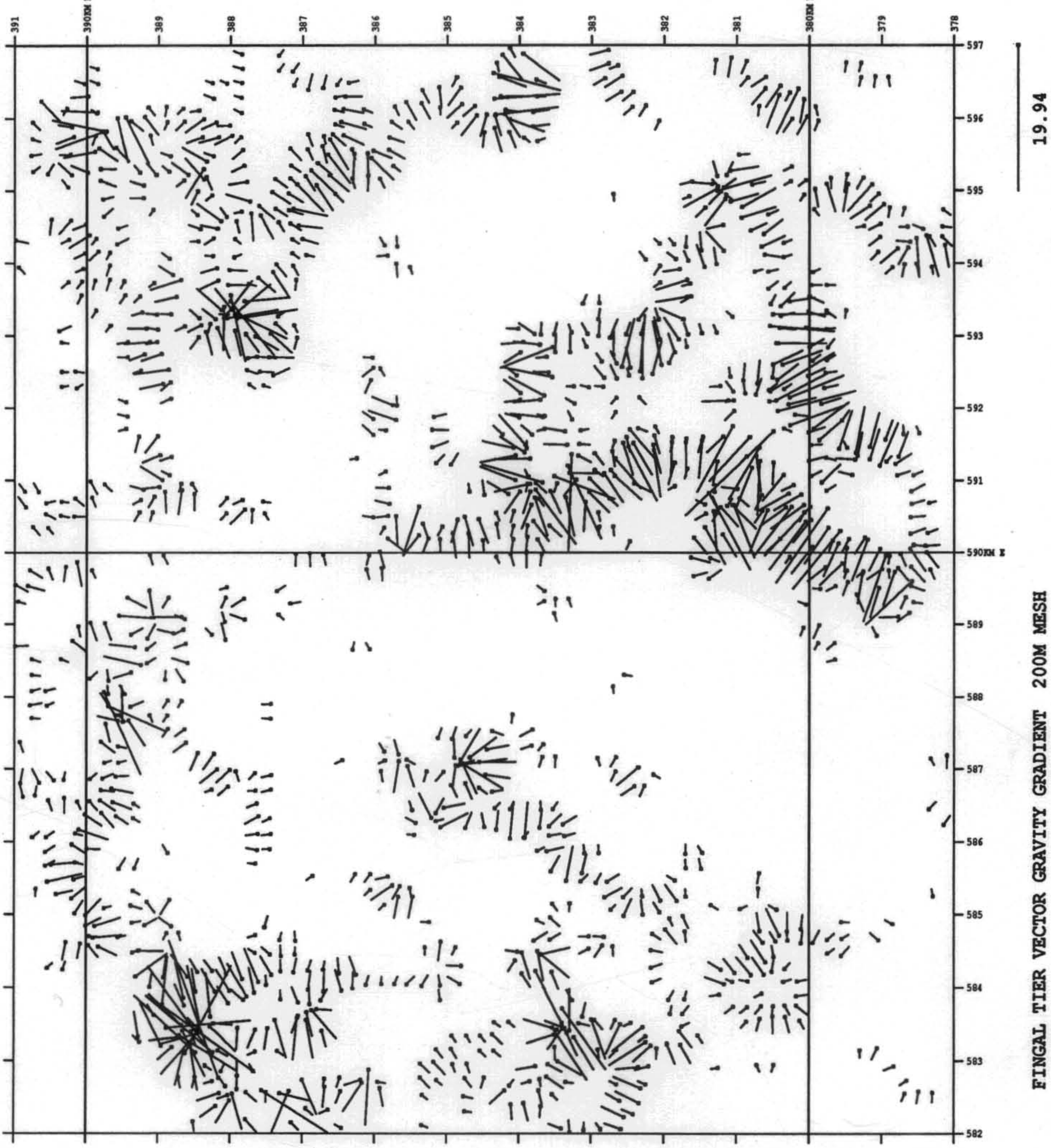

Figure 37
Vector gravity gradient, Fingal Tier (200 m mesh)

5 cm

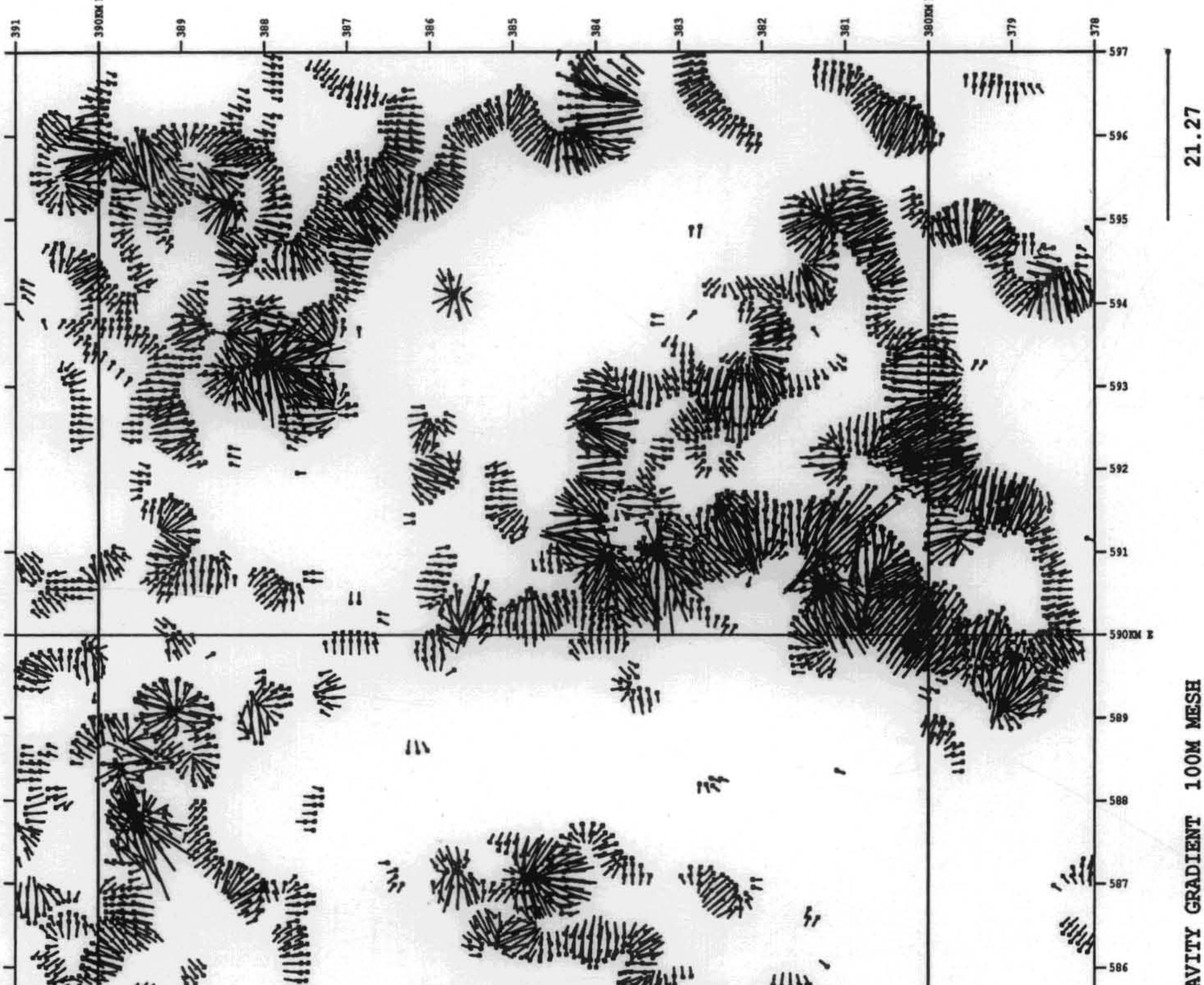

Figure 38

Vector gravity gradient, Fingal Tier (100 m mesh)